Available online at www.sciencedirect.com
SCIENCE DIRECT®
Coordination Chemistry Reviews 249 (2005) 591–612
COORDINATION CHEMISTRY REVIEWS
www.elsevier.com/locate/ccr

Review

# Structural and spectroscopic properties of dinuclear rhenium complexes containing $(ReO)_2(\mu\text{-}O)$ core

B. Machura*

*Department of Inorganic and Radiation Chemistry, Institute of Chemistry, University of Silesia, 9th Szkolna St., 40-006 Katowice, Poland*

Received 11 May 2004; accepted 6 July 2004
Available online 18 September 2004

## Contents



**Abstract**

This paper investigates the structural and spectroscopic properties of dinuclear rhenium complexes containing $(ReO)_2(\mu\text{-}O)$ core. Some aspects connected with methods of synthesis are also discussed here. Considering the structure of Re─O─Re bridge, these compounds have been generally divided into two groups: (i) complexes with a linear Re─O─Re unit, and (ii) complexes with a bent Re─O─Re core.


*Keywords:* Rhenium complexes; Dinuclear complexes; Oxo compounds

## 1. Introduction

Recent interest in the coordination chemistry of rhenium arises mainly from the introduction of $\beta^-$ emitting isotopes $^{188}Re$ and $^{186}Re$ in radiotherapy and its similarity with technetium, whose metastable $\gamma$-emitting isotope $^{99m}Tc$ plays important role in diagnostic nuclear medicine. The success of the $^{186}Re(Sn)HEDP$ radiopharmaceutical as a palliative of bone pain has particularly reawakened interest in the coordination chemistry of rhenium in order to develop new $^{186/188}Re$ radiopharmaceuticals which could be used for the treatment of cancer [1–6].

Rhenium(V) complexes comprise a prominent class of compounds in radiopharmaceutical chemistry. The oxidation V of rhenium is easily stabilized by a large variety of ligands

* Tel.: +48 32252441; fax: +48 322599978.
*E-mail address:* bmachura@poczta.onet.pl.

0010-8545/$ – see front matter © 2004 Elsevier B.V. All rights reserved.
doi:10.1016/j.ccr.2004.07.007

**Nomenclature**

$acac_2enH_2$ *N*,*N*′-ethylenebis(acetylacetimine)
$biimH_2$ biimidiazole

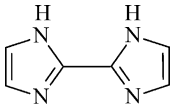

$biimMe_2$ *N*,*N*′-dimethylbiimidiazole
$bpaO_2H$ 1,3-*bis*(2-piridyl)-2-azapropanedione

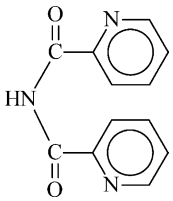

dioxo-$tetH_6$ 1,4,8,11-tetraazaundecane-5,7-dione

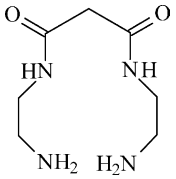

dippm di(isopropylphosphino)methane
dmpn-sal *N*,*N*′-2,2-dimethylpropane-1,3-diylbis(salicylideneimine)

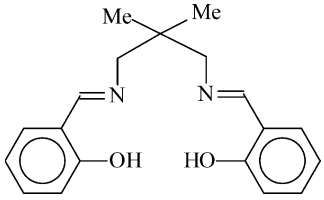

dppm di(phenylphosphino)methane
eami 2-(1-ethylaminomethyl)-1-methylimidiazole

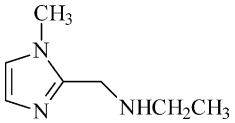

etmi 2-(1-ethylthiomethyl)-1-methylimidiazole

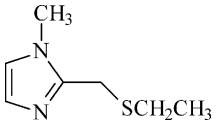

$HB(pz)_3$ hydrotris(1-pyrazoyl)borate
HEDP hydroxyethylenediphosphonic acid
hisMe histidine methyl ester
$HL^1$ [1-(thiazol-2-ylcarbamoyl)-ethyl]-carbamic acid benzyl ester

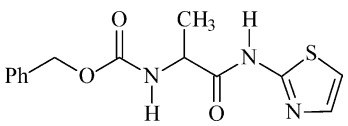

$HL^2$ [2-phenyl-1-(thiazol-2-ylcarbamoyl)-ethyl]-carbamic acid benzyl ester

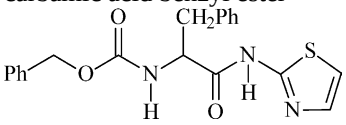

$HL^3$ [2-phenyl-1-(thiazol-2-ylcarbamoyl)-ethyl]-carbamic acid *tert*-butyl ester

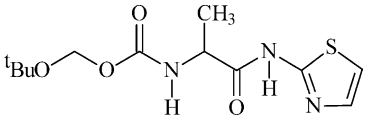

mami 2-(1-methylaminomethyl)-1-methylimidiazole

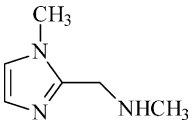

1-Meim 1-methylimidiazole
$Me_2pymSH$ 4,6-dimethylpyrimidine-2(H)-thione

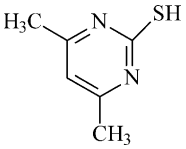

$Me_3Bzm$ 1,5,6-trimethylbenzimidiazole
3,4-lut 3,5-lutidine
pzH pyrazole
Pym pyrimidine
Pyz pyrazine
$sal_2enH_2$ *N*,*N*′-ethylenebis(salicylideneimine)

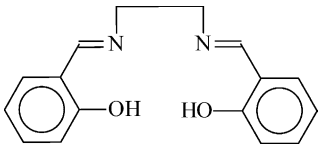

$salpdH_2$ *N*,*N*′-propane-1,3-diylbis(salicylideneamine)

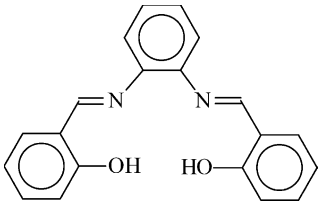

$sal_2phenH_2$ *N*,*N*′-trimethylene *bis*(salicylideneimine)

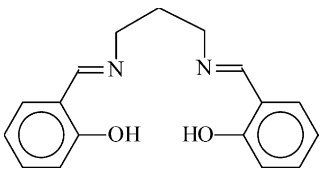

$tppH_2$ 5,10,15,20-tetraphenylporphyrine

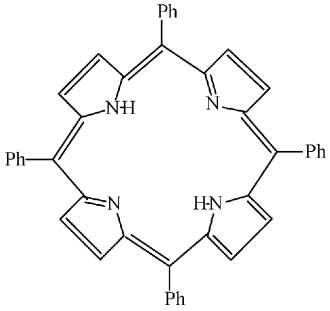

$N_2O_2$-calix[4]arene

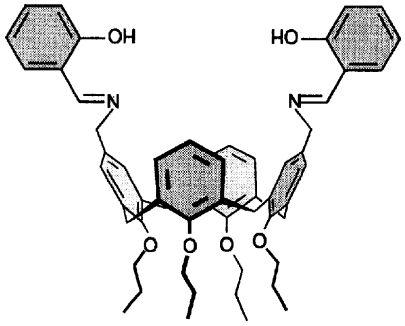

and it is easily obtained from the reduction of perrhenate. A distinctive feature of most stable Re(V) complexes is the existence of multiple bonds to sulfur, nitrogen and especially oxygen [7,8].

Oxorhenium(V) complexes have been known for many years and the Re=O core has attracted much attention due to its spectroscopic properties, basicity towards various Lewis acids, influence on ligand distributions in coordination sphere, role in oxygen transfers and catalytic processes [9–11].

This paper is a review on the preparations, structures and properties of dinuclear rhenium complexes containing $(ReO)_2(\mu\text{-}O)$ core. Considering the structure of Re–O–Re bridge, these compounds can be divided into two groups: (i) complexes with a linear Re–O–Re core, and (ii) complexes with a bent Re–O–Re bridge. The terminal oxo ligands may take different arrangement towards a linear Re–O–Re bridge to give: complexes with a linear O=Re–O–Re=O backbone (a), complexes with a linear Re–O–Re unit and *trans* terminal oxo ligands arrangement (b), and complexes with a linear Re–O–Re unit and *cis* terminal oxo ligands arrangement (c).

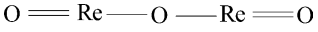

(a)

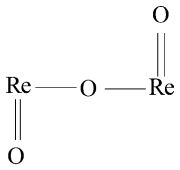

(b)

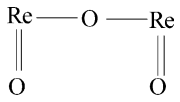

(c)

For rhenium, the complexes with a linear Re–O–Re unit and *cis* terminal oxo ligands arrangement have not been isolated, and dinuclear $(ReO)_2(\mu\text{-}O)$ compounds with *trans* geometry of the terminal oxo ligands are very sparse. Although the complexes with a linear O=Re–O–Re=O backbone and the complexes with a linear Re–O–Re unit and *trans* terminal oxo ligands arrangement generally belong to the same group, they have been discussed separately in the Sections 2 and 4, respectively.

## 2. Dinuclear rhenium complexes with a linear O=Re–O–Re=O backbone

### 2.1. Structural properties

$[\{ReOCl_2(py)_2\}_2(\mu\text{-}O)]$ was the first structurally characterised dinuclear rhenium(V) complex with essentially linear oxo-bridged O=Re–O–Re=O backbone. The *cis*,*cis* arrangement of pyridines in the $ReCl_2N_2$ planes seemed to be uncommon for a coordination sphere of such composition, since the $[ReO(OR)Cl_2L_2]$ complexes, in particular $[ReO(OEt)Cl_2(py)_2]$, adopted the *trans*,*trans* arrangement. Lock and Turner analysed the possible conformations of $[\{ReOCl_2(py)_2\}_2(\mu\text{-}O)]$ based on idealized structures and normal values for bond lengths and van der Waals radii. The calculations showed that the anomalies in $[\{ReOCl_2(py)_2\}_2(\mu\text{-}O)]$ could be explained in terms of the intramolecular packing requirements of the pyridine rings [12].

A *cis*,*cis* geometry of hetrocyclic molecules in the $ReCl_2L_2$ planes was confirmed later in many other rhenium complexes of the $[\{ReOX_2L_2\}_2(\mu\text{-}O)]$ type [13–17].

In the case of different ligands $L_1$ and $L_2$, a racemic mixture of AA or CC enantiomeric dimers and a *meso* (AC) dimer are expected (Scheme 1).

Table 1 presents the Re–$O_t$ and Re–$O_b$ bond lengths [Å] and $O_t$–Re–$O_b$ and Re–$O_b$–Re angles [°] of the $[\{ReOX_2L_2\}_2(\mu\text{-}O)]$ compounds. All the structurally characterised $[\{ReOX_2L_2\}_2(\mu\text{-}O)]$ complexes present a nearly linear O=Re–O–Re=O unit with the rhenium atoms in a pseudo-octahedral coordination environment. The dihedral

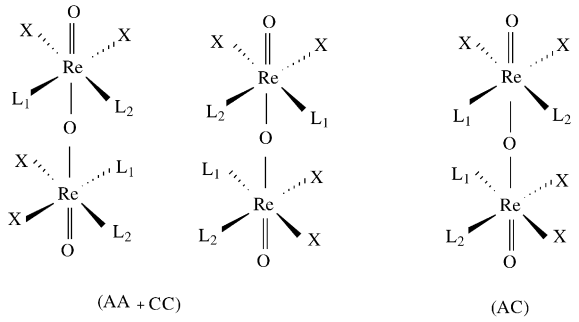


Scheme 1. For simplicity, the eclipsed forms of the dimmers are shown.

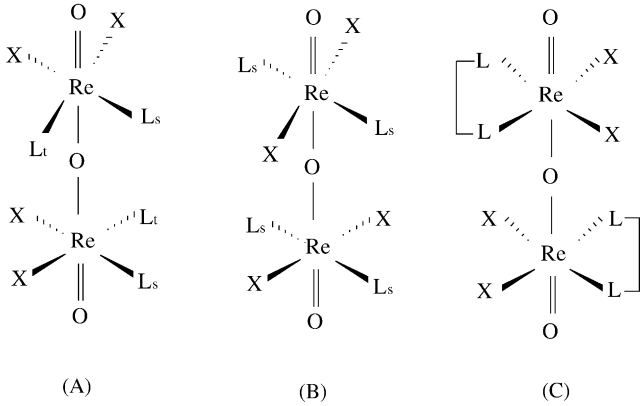


Scheme 2.

angles between the *N*-heterocyclic ligands L and the $ReX_2L_2$ planes are 37°–58°, what minimizes short contacts around the Re=O and Re–X bonds. The $OReX_2L_2$ units are rotated 23°–33° about the Re–Re axis away from an eclipsed conformation (Scheme 2A). This arrangement avoids short contacts between the L ligands in different halves of the dimer and allows some stacking to take place between the $L_s$ ligands.

The twist angle depends on steric requirements of the heterocyclic ligands. It is equal 23° for the $[Re_2O_3Cl_4py_4]$ complex [12] but in the $[\{Re(O)Cl_2(3,5\text{-}Me_2pzH)_2\}_2(\mu\text{-}O)]$ containing much more bulky heterocyclic molecules is 32.52° [14]. A thermal ellipsoid plot of $[\{Re(O)Cl_2(3,5\text{-}Me_2pzH)_2\}_2(\mu\text{-}O)]$ is shown in Fig. 1. The $[\{Re(O)Cl_2(3,5\text{-}Me_2pzH)_2\}_2(\mu\text{-}O)]$ complex has a pseudo two-fold axis going through O(1) atom and midpoint of distance linking the Cl(2) and Cl(3) atoms (total root mean square deviation of superposed monomers for all nonhydrogen atoms is 0.0930 Å), and the main difference exists in the positions of the hydrogen atoms of the methyl groups.

Rotation of the two halves of *rac*-$[\{ReOCl_2(Me_3Bzm)(py)\}_2(\mu\text{-}O)]$ and *meso*-$[\{ReOCl_2(Me_3Bzm)(3,4\text{-lut})\}_2(\mu\text{-}O)]$ dimers about the Re–Re vector away from an eclipsed conformation allows stacking of the pyridines in *rac*-$[\{ReOCl_2(Me_3Bzm)(py)\}_2(\mu\text{-}O)]$ and the 3,5-lut/$Me_3Bzm$ pair in *meso*-$[\{ReOCl_2(Me_3Bzm)(3,4\text{-lut})\}_2(\mu\text{-}O)]$ [17].

The $[\{ReOX_2L_2\}_2(\mu\text{-}O)]$ complexes with a *trans* arrangement of monodentate ligands L in the $ReX_2L_2$ planes have also been characterised [19,20]. The Re–$O_t$ and Re–$O_b$ bond lengths [Å] and $O_t$–Re–$O_b$ and Re–$O_b$–Re angles [°] for the $[\{Re(O)Cl_2(1\text{-MeIm})_2\}_2(\mu\text{-}O)]$ and $[\{Re(O)Cl_2(py)_2\}_2$

Table 1
The selected bond lengths [Å] and angles [°] for the $[\{ReOX_2L_2\}_2(\mu\text{-}O)]$ compounds with the *cis,cis* and *trans,trans* geometries of monodentate ligands in the $ReCl_2L_2$ planes

| Complex | Re–$O_t$ | Re–$O_b$ | $O_t$–Re–$O_b$ | Re–$O_b$–Re | Ref. |
|---|---|---|---|---|---|
| *cis,cis* | | | | | |
| $[\{ReOCl_2(py)_2\}_2(\mu\text{-}O)]$ | 1.764(16) | 1.903(16) | 165.5(7) | 174.5(9) | [12] |
| | 1.715(16) | 1.943(16) | 172.8(7) | | |
| $[\{ReOCl_2(Me_2pzH)_2\}_2(\mu\text{-}O)]\cdot Me_2CO$ | 1.694(7) | 1.921(6) | 172.5(3) | 177.7(4) | [13] |
| | 1.685(7) | 1.937(6) | 173.5(3) | | |
| $[\{ReOCl_2(Me_2pzH)_2\}_2(\mu\text{-}O)]$ | 1.682(4) | 1.933(3) | 171.9(2) | 178.0(2) | [14] |
| | 1.678(4) | 1.918(3) | 172.7(2) | | |
| $[\{ReOBr_2(Me_2pzH)_2\}_2(\mu\text{-}O)]$ | 1.686(4) | 1.946(3) | 172.4(2) | 178.7(2) | [14] |
| | 1.681(4) | 1.925(3) | 173.0(2) | | |
| $[\{ReOCl_2(pyz)\}_2(\mu\text{-}O)]$ | 1.706(7) | 1.921(5) | 168.0(3) | 179.0(3) | [15] |
| | 1.688(7) | 1.926(5) | 167.3(3) | | |
| $[\{ReOCl_2(Me_3Bzm)_2\}_2(\mu\text{-}O)]\cdot 2Me_2CO$ | 1.696 | 1.941 | 170.4 | 176.3 | [16] |
| | 1.688 | 1.909 | 172.3 | | |
| *rac*-$[\{ReOCl_2(Me_3Bzm)(py)\}_2(\mu\text{-}O)]$ | 1.671(7) | 1.915(7) | 170.0(3) | 176.9(5) | [17] |
| *meso*-$[\{ReOCl_2(Me_3Bzm)(3,4\text{-lut})\}_2(\mu\text{-}O)]$ | 1.669(7) | 1.899(7) | 170.2(3) | 175.1(4) | [17] |
| | 1.683(7) | 1.923(7) | 168.6(3) | | |
| $[\{ReOCl_2(2,6\text{-}(CH_3)_2\text{-}C_6H_3NC)\}_2(\mu\text{-}O)]$ | 1.692(7) | 1.9050(8) | 168.8(3) | 174.5(6) | [18] |
| Mean | 1.692 | 1.923 | | | |
| *trans,trans* | | | | | |
| $[\{ReOCl_2(1\text{-Meim})_2\}_2(\mu\text{-}O)]$ | 1.703(8) | 1.913(1) | 180 | 180 | [19] |
| $[\{ReOCl_2(py)_2\}_2(\mu\text{-}O)]$ | 1.681(7) | 1.933(5) | 177.9(3) | 178.4(3) | [20] |
| | 1.671(7) | 1.912(5) | 177.3(3) | | |
| Mean | 1.685 | 1.919 | | | |

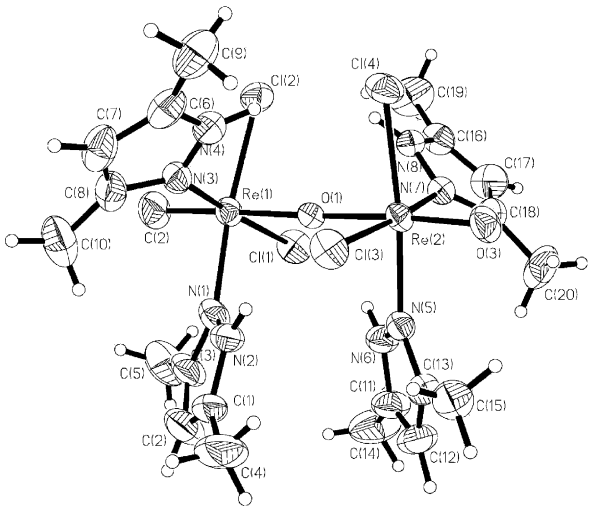


Fig. 1. Structure of $[\{Re(O)Cl_2(3,5\text{-}Me_2pzH)_2\}_2(\mu\text{-}O)]$ [14].

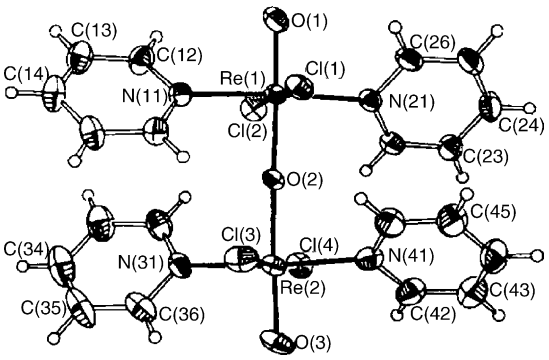


Fig. 2. Structure of *trans,trans*-$[\{Re(O)Cl_2(py)_2\}_2(\mu\text{-}O)]$ [20].

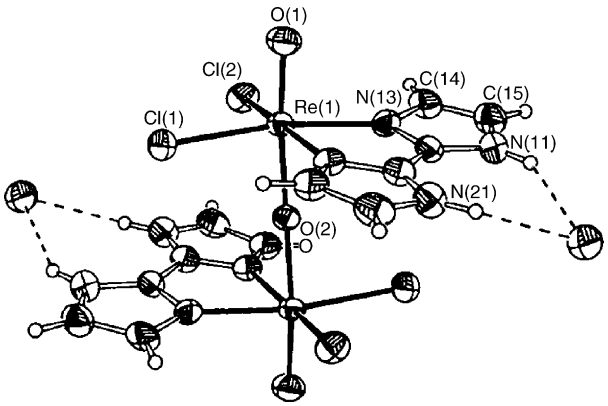


Fig. 3. Structure of $[\{OReCl_2(biimH_2\cdots Cl)\}_2(\mu\text{-}O)]^{2-}$ unit [25].

(μ-O)] with *trans,trans* geometry of the heterocyclic molecules are presented in Table 1. The O=Re–O–Re=O backbone in $[\{Re(O)Cl_2(1\text{-}MeIm)_2\}_2(\mu\text{-}O)]$ is perfectly linear; the bridging O atom occupies a site of crystallographic 222 symmetry, and the rhenium and the terminal atoms lie on one of these two-fold axes. The O=Re–O–Re=O unit of the pyridine complex is almost linear. The dihedral angles between the heterocyclic ligands L and the $ReX_2L_2$ plane are 37°–51° in the *trans,trans*-$[\{ReOX_2L_2\}_2(\mu\text{-}O)]$ complexes. The $OReCl_2L_2$ units are rotated about the Re–Re axis away from an eclipsed arrangement and twist angles for $[\{Re(O)Cl_2(1\text{-}MeIm)_2\}_2(\mu\text{-}O)]$ and $[\{Re(O)Cl_2(py)_2\}_2(\mu\text{-}O)]$ are equal 29° and 27.3°, respectively. This conformation allows stacking interactions to occur between the two pairs of heterocyclic ligands (Scheme 2B). Fig. 2 presents a perspective drawing of the *trans,trans*-$[\{Re(O)Cl_2(py)_2\}_2(\mu\text{-}O)]$ complex [20].

In dirhenium complexes containing a linear O=Re–O–Re=O unit and bidentate ligands (L–L), the configuration is necessarily *cis* (Scheme 2C). The halogene and bidentate ligands are placed in an *anti* position with respect to the bridging oxygen. Table 2 presents the $Re–O_t$ and $Re–O_b$ bond lengths [Å] and $O_t–Re\text{-}O_b$ and $Re–O_b–Re$ angles [°] of the $[\{ReOX_2(L–L)\}_2(\mu\text{-}O)]$ compounds [21–26]. For the $[\{ReOCl_2(en)\}_2(\mu\text{-}O)]$ [22], $[\{ReOCl_2(etmi)\}_2(\mu\text{-}O)]$ [21] and $[\{ReOCl_2(biimH_2)\}_2(\mu\text{-}O)](PPh_4Cl)_2{\cdot}2H_2O$ [25] complexes, the bridging oxygen atom sits on an inversion centre and a perfectly eclipsed conformation is observed. In the complexes with thiolate, L-histidine and 2-(1-ethylaminomethyl)-1-methylimidiazole ligands the deviations from the eclipsed conformations are small; the halogene ligands of one $ReX_2(L–L)$ unit almost

Table 2
The selected bond lengths [Å] and angles [°] for the $[\{ReOX_2(L–L)\}_2(\mu\text{-}O)]$ complexes

| Complex | $Re–O_t$ | $Re–O_b$ | $O_t–Re–O_b$ | $Re–O_b–Re$ | Ref. |
|---|---|---|---|---|---|
| $[\{ReOCl_2(eami)\}_2(\mu\text{-}O)]$ | 1.676(6) | 1.905(5) | 167.5(3) | 176.4(3) | [21] |
| | 1.684(6) | 1.905(5) | 168.7(3) | | |
| $[\{ReOCl_2(etmi)\}_2(\mu\text{-}O)]$ | 1.687(4) | 1.9267(2) | 169.68(12) | 180 | [21] |
| $[\{ReOCl_2(en)\}_2(\mu\text{-}O)]$ | 1.666(47) | 1.912(5) | 172.9(16) | 180 | [22] |
| $[\{ReOCl_2(AcO(CH_2)_2S(CH_2)_2S(CH_2)_2OAc)\}_2(\mu\text{-}O)]$ | 1.72(2) | 1.88(2) | 167.3(1) | 175.3(2) | [23] |
| | 1.67(2) | 1.97(2) | 167.7(2) | | |
| $[\{ReOCl_2(Bu^nSCH_2CH_2SBu^n)\}_2(\mu\text{-}O)]$ | 1.705(8) | 1.908(9) | 168.1(4) | | [24] |
| | 1.735(4) | 1.946(9) | 158.6(5) | | |
| $[\{ReOCl_2(biimH_2)\}_2(\mu\text{-}O)](PPh_4Cl)_2\cdot 2H_2O$ | 1.693(5) | 1.9047(6) | 173.6(2) | 180 | [25] |
| $[\{ReOBr_2(L\text{-}hisMe)\}_2(\mu\text{-}O)]$ | 1.677(12) | 1.913(1) | 169.4(1) | 178.2(1) | [26] |
| | 1.715(15) | 1.912(1) | 171.6(1) | 178.6(2) | |
| Mean | 1.693 | 1.917 | | | |

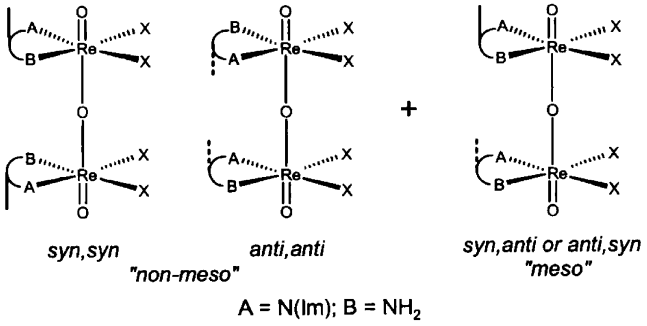


Scheme 3.

eclipse the sulfur or nitrogen atoms of the other part of the molecule (torsion angles are between 2.4° and 5.4°). The unit cell of the complex with biimidiazole contains two $Cl^-$ and two $PPh_4^+$ ions per dinuclear molecule. The $Cl^-$ ion is hydrogen-bonded to the N–H groups of each $biimH_2$ ligand. Therefore, the structure can be described as the *bis*-$PPh_4^+$ salt of the tightly associated $[\{ORECl_2(biimH_2\ldots Cl)\}_2(\mu\text{-}O)]^{2-}$ unit, presented in Fig. 3 [25].

An achiral A–B bidentate ligand should produce a *meso* isomer and a pair of enantiomers. The presence of asymmetric carbon in L-histidine ligand increases the number of possible isomers (Scheme 3), the proton on the chiral centre can be *syn* or *anti* with respect to the Re=O bond. For $[\{ReOBr_2(L\text{-}hisMe)\}_2(\mu\text{-}O)]$ only the two *non-meso* species are observed in the solid state and solution. It is probably connected with additional stabilization of these forms by hydrogen bonds [26].

Table 3 presents the Re–$O_t$ and Re–$O_b$ bond lengths [Å] and $O_t$–Re–$O_b$ and Re–$O_b$–Re angles [°] for the complexes of general composition $[\{ReO(L_4)\}_2(\mu\text{-}O)]$ ($L_4$ = two bidentate ligands or one tetradentate ligand) [27–34]. The two moieties of $[ReO(acac)\{\eta^2\text{-}B(pz)_4\}]_2(\mu\text{-}O)$ are bridged by the oxygen atom lying on a centre of symmetry and imposing a strictly linear Re–O–Re bridge [30]. The bridging oxygen atom of $[\{ReO(Me_2pymS)_2\}_2(\mu\text{-}O)]$ lies on a site of mm crystallographic symmetry and the rhenium and the terminal oxygen atoms on one of these mirror planes. The ligand molecules of $[\{ReO(Me_2pymS)_2\}_2(\mu\text{-}O)]$ are found to be disordered with about 50% occupancy of two different positions with pivot around the C(1)–N(2) bond. In both configurations the pairs of nitrogen and sulphur atoms of the equatorial donor set are *cis*-arranged around the rhenium ion in each half of the dimer and for both configurations the equatorial ligands in one half of the dimer are eclipsed with respect to the corresponding other half [29]. A perspective view of the $[\{ReO(Me_2pymS)_2\}_2(\mu\text{-}O)]$ dimer along the O=Re–O–Re=O backbone showing the two disordered position of the ligand is depicted in Fig. 4.

The diethyldithiocarbamato-ligands of $[\{Re(S_2CNEt_2)_2\}_2(\mu\text{-}O)]$ attached to the two metal atoms are staggered

Table 3
The selected bond lengths [Å] and angles [°] for the $[\{ReO(L_4)\}_2(\mu\text{-}O)]$ complexes

| Complex | Re—$O_t$ | Re—$O_b$ | $O_t$—Re—$O_b$ | Re—$O_b$—Re | Ref. |
|---|---|---|---|---|---|
| $[\{ReO(S_2CNEt_2)_2\}_2(\mu\text{-}O)]$ | 1.723(7) | 1.917(5) | 177.9(3) | 175.5(3) | [27] |
| | 1.721(7) | 1.903(5) | 173.8(3) | | |
| $[\{ReO(SCH_2CH_2NHCH_2CH_2SEt)_2\}_2(\mu\text{-}O)]$ | 1.713(6) | 1.932(5) | 156.4(3) | 160.8(3) | [28] |
| | 1.703(6) | 1.949(5) | 156.6(3) | | |
| $[\{ReO(Me_2pymS)_2\}_2(\mu\text{-}O)]$ | 1.688(7) | 1.915(5) | 179.4(3) | 178.7(4) | [29] |
| $[ReO(acac)\{\eta^2\text{-}B(pz)_4\}]_2(\mu\text{-}O)$ | 1.663(10) | 1.910(1) | 175.6(4) | 180 | [30] |
| $[\{ReO(salpd)\}_2(\mu\text{-}O)]$, $(P2_1/c)$ | 1.699 | 1.912 | 180 | 180 | [31] |
| | 1.707 | 1.915 | | | |
| $[\{ReO(salpd)\}_2(\mu\text{-}O)]$, $(P2_1/c)$ | 1.712(4) | 1.9152(7) | 168.63(12) | 180 | [32] |
| $[\{ReO(salpd)\}_2(\mu\text{-}O)]$, (Pbca) | 1.694(8) | 1.9130(6) | 168.5(3) | 180 | [32] |
| $[\{ReO(salpd)\}_2(\mu\text{-}O)]\cdot 4CHCl_3$ | 1.696(12) | 1.919(2) | 168.4(3) | 180 | [32] |
| $[\{ReO(salpd)\}_2(\mu\text{-}O)]\cdot 2CHCl_3$ | 1.699(4) | 1.9106(4) | 168.32(14) | 180 | [32] |
| $[\{ReO(salpd)\}_2(\mu\text{-}O)]\cdot 2CH_2Cl_2$ | 1.697(5) | 1.9090(6) | 166.81(17) | 180 | [32] |
| $[\{ReO(salpd)\}_2(\mu\text{-}O)]\cdot 2H_2O$ | 1.724(7) | 1.9129(3) | 165.92(18) | 180 | [32] |
| $[\{ReO(dmpn\text{-}sal)\}_2(\mu\text{-}O)]$ | 1.697(4) | 1.9114(2) | 171.76(14) | 180 | [33] |
| $[\{ReO(tpp)\}_2(\mu\text{-}O)]$ | 1.704 | 1.948 | 180 | 180 | [34] |
| | 1.728 | 1.894 | | | |
| $[\{ReO(dioxo\text{-}tetH_4)\}_2(\mu\text{-}O)]\cdot 4H_2O$ | 1.698(3) | 1.9342(4) | 166.50(14) | 173.4(2) | [35] |
| | 1.677(3) | 2.185(3) | 166.74(13) | | |
| $[\{ReO(N_2O_2\text{-}calix[4]arene)\}_2(\mu\text{-}O)]$ | 1.703 | 1.919 | 176.7 | 177.3 | [36] |
| | 1.695 | 1.926 | 179.1 | | |
| $[\{ReO\{N,N'\text{-}bis(2\text{-hydroxybenzyl})\text{-}1,3\text{-diaminopropane}\}_2]$ $(\mu\text{-}O)$ | 1.692(13) | 1.908(12) | 166.6(7) | 169.2(9) | [37] |
| | 1.656(15) | 1.942(12) | | | |
| $[\{ReO\{N,N'\text{-}bis(2\text{-hydroxybenzyl})\text{-}1,3\text{-diaminobutane}\}_2]$ $(\mu\text{-}O)$ | 1.698(7) | 1.924(6) | 165.8(4) | 165.8(4) | [37] |
| | 1.699(7) | 1.942(6) | | | |
| $[\{ReO\{N,N'\text{-}bis(2\text{-hydroxyacetobenzyl})\text{-}1,3\text{-diaminopropane}\}_2]$ $(\mu\text{-}O)$ | 1.687(10) | 1.9367(9) | 163.3(4) | 180 | [37] |
| $[\{ReO\{N,N'\text{-}bis(2\text{-hydroxybenzyl})\text{-}1,3\text{-diamino-2-(4-nitrobenzyl)propane}\}_2]$ $(\mu\text{-}O)$ | 1.700 | 1.927 | 162.6 | 180 | [34] |
| Mean | 1.699 | 1.931 | | | |

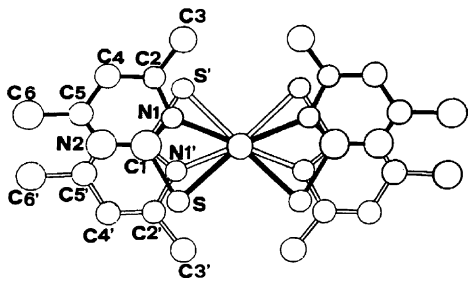


Fig. 4. Perspective view of the [{ReO(Me$_2$pymS)$_2$}$_2$(μ-O)] dimer along the O=Re—O—Re=O backbone showing the two disordered position of the ligand [29].

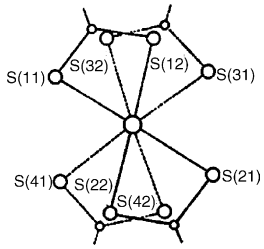


Fig. 5. A schematic view of [{Re(S$_2$CNEt$_2$)$_2$}$_2$(μ-O)] along the O=Re—O—Re=O backbone showing the degree of staggering of diethyldithiocarbamato-ligands [27].

by ca. 40° relative to each other [27]. Fig. 5 presents a schematic view of [{Re(S$_2$CNEt$_2$)$_2$}$_2$(μ-O)] along the O=Re–O–Re=O backbone.

Seven crystal structures of polymorphs and pseudo-polymorhps of [{ReO(salpd)}$_2$(μ-O)] were obtained during the study of the configurational control of rhenium(V)-*bis*(salicylidene)alkanediamine complexes [32]. The protruding methylene units of both independent salpd ligands can point away from the inversion-related ligand with which the dinuclear complex is formed, leaving the six-membered *N*,*N*-chelate ring in an envelope conformation ('open' conformation) or point towards the inversion-related ligand ('closed' conformation). The 'open' and 'closed' conformations of [{ReO(salpd)}$_2$(μ-O)] are depicted in Figs. 6 and 7, respectively.

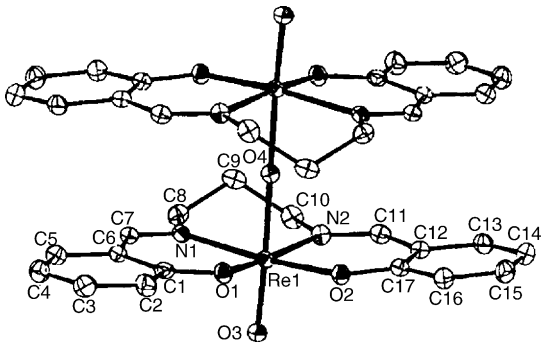


Fig. 7. The 'closed' conformation of [{ReO(salpd)}$_2$(μ-O)] [32].

In the orthorhombic polymorph of [{ReO(salpd)}$_2$(μ-O)], the open and closed conformations occur in a disordered fashion (Fig. 8). The intra and intermolecular interactions of polymorphs and pseudo-polymorphs of [{ReO(salpd)}$_2$(μ-O)] have been discussed in detail in the papers [31,32].

The Re–O$_t$ and Re–O$_b$ bond lengths [Å] and O$_t$–Re–O$_b$ and Re–O$_b$–Re angles [°] of the other dirhenium complexes containing a linear O=Re–O–Re=O backbone [38–42] are gathered in Table 4.

The longest Re–O$_t$ distance (1.764(16) Å) is observed in the case of the *cis*,*cis*-[{ReOCl$_2$(py)$_2$}$_2$(μ-O)], but this value is rather questionable — the final refinement was not satisfactory for this oxocomplex [12]. No significant differences in the Re–O$_t$ distances are noticed for complexes with mono-, bi- and tetradendante ligands. The average Re–O$_t$ bond lengths are equal 1.692, 1.685, 1.693 and 1.699 Å for *cis*,*cis*-[{ReOX$_2$L$_2$}$_2$(μ-O)], *trans*,*trans*-[{ReOX$_2$L$_2$}$_2$(μ-O)], [{ReOX$_2$(L–L)}$_2$(μ-O)] and [{ReO(L$_4$)}$_2$(μ-O)], respectively. The mean Re–O$_t$ bond length found for [{ReOX$_2$L$_2$}$_2$(μ-O)] complexes with *trans* geometry of the monodentate ligands L is somewhat shorter in comparison with the one observed for *cis*,*cis*-[{ReOX$_2$L$_2$}$_2$(μ-O)], but the number of *trans*,*trans*-[{ReOX$_2$L$_2$}$_2$(μ-O)] is too small to discuss the difference between them. For comparison, the average rhenium–oxygen

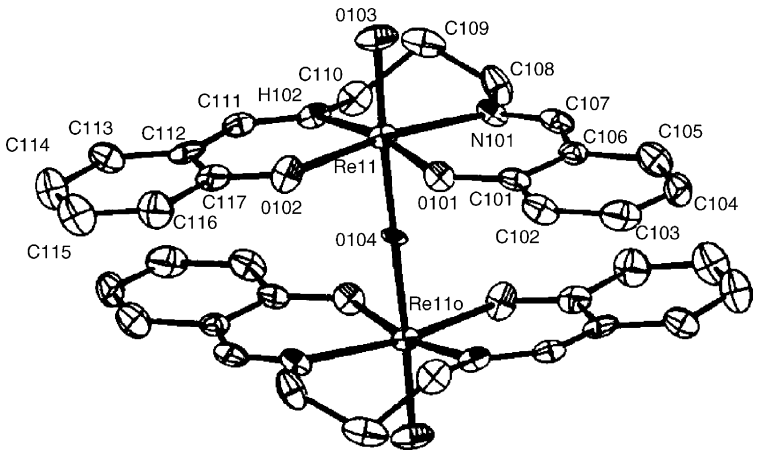


Fig. 6. The 'open' conformation of [{ReO(salpd)}$_2$(μ-O)] [31].

Table 4
The selected bond lengths [Å] and angles [°] for the other dirhenium complexes with the linear -O=Re—O—Re=O backbone

| Complex | Re—$O_t$ | Re—$O_b$ | $O_t$—Re—$O_b$ | Re—$O_b$—Re | Ref. |
|---|---|---|---|---|---|
| $K_3Na[\{ReO(CN)\}_4(\mu\text{-}O)]\cdot 2H_2O$ | 1.732(11) | 1.934(1) | 180 | 180 | [38] |
| $[\{ReO(BiimH_2)_2\}_2(\mu\text{-}O)]Cl_4\cdot 6H_2O$ | 1.65(2) | 1.92(3) | 180 | 180 | [39] |
| | 1.74(2) | 1.89(3) | | | |
| $[\{ReO(SCH_2CH_2NHCH_2CH_2SEt)(S\}_2(\mu\text{-}O)]$ | 1.707(5) | 1.934(1) | 159.6(2) | 180 | [28] |
| $[\{ReOCl(bpaO_2)\}_2(\mu\text{-}O)]\cdot 2MeCN$ | 1.700(3) | 1.9122(1) | | 180 | [40] |
| $[\{ReOCl_2\}_2(\mu\text{-}O)(\mu\text{-dppm})_2]\cdot Me_2CO$ | 1.708(6) | 1.9115(5) | 178.1(2) | 180 | [41] |
| $[\{ReOCl_2\}_2(\mu\text{-}O)(\mu\text{-dppm})_2]\cdot CH_2Cl_2$ | 1.68(1) | 1.9097(7) | 175.3(4) | 180 | [41] |
| $[\{ReOCl_2\}_2(\mu\text{-}O)(\mu\text{-dippm})_2]$ | 1.708(9) | 1.921(8) | 178.9(4) | 179.8(5) | [42] |
| | 1.705(10) | 1.904(8) | 179.5(4) | | |
| Mean | 1.703 | 1.915 | | | |

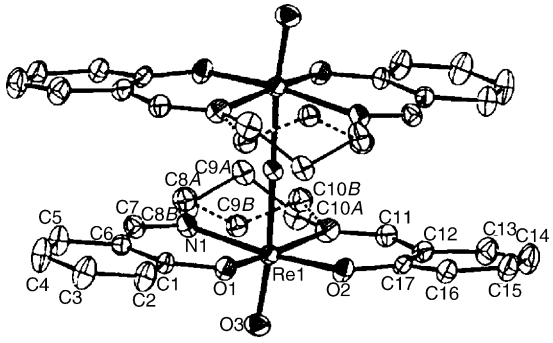


Fig. 8. Structure of orthorhombic polymorph of $[\{ReO(salpd)\}_2(\mu\text{-}O)]$ [32].

bond lengths in mono-, di- and tri-oxo mononuclear complexes are 1.686, 1.734 and 1.708 Å, respectively [43].

The average Re–$O_b$ distances are 1.921, 1.917 and 1.931 Å for $[\{ReOX_2L_2\}_2(\mu\text{-}O)]$, $[\{ReOX_2(L\text{–}L)\}_2(\mu\text{-}O)]$ and $[\{ReO(L_4)\}_2(\mu\text{-}O)]$, respectively. An insignificant lengthening of Re–$O_b$ bond lengths is observed for the $[\{ReO(L_4)\}_2(\mu\text{-}O)]$ complexes. In comparison with the Re–$O_b$ bond lengths of the complexes containing only bridging oxygen, all they are considerable longer: 1.844 Å in $[\{Re_2Cl(phen)_2\}(\mu\text{-}O)]^{2+}$ [44] and 1.830 in $[Re_2Cl_6(\mu\text{-}dppe)_2(\mu\text{-}O)]$ [41].

### 2.2. The electronic structure

The electronic structures of $[\{Re(O)Br_2(3,5\text{-}Me_2pzH)_2\}_2(\mu\text{-}O)]$ and model compound — $[\{Re(O)Br_2(NH_3)_2\}_2(\mu\text{-}O)]$ were examined using the density functional theory (DFT) [45]. The rhenium atoms of the investigated complexes possess $d^2$ electronic configuration. Two highest occuppied MOs of $[\{Re(O)Br_2(3,5\text{-}Me_2pzH)_2\}_2(\mu\text{-}O)]$ are $d_{xy}$ with an antibonding contributions from $p_\pi$ bromine orbitals. The remaining eight d-type orbitals of rhenium are found among unoccuppied MOs, some of them bear antibonding character towards the oxygen atoms. Fig. 9 presents the energy and contours of the occupied and unoccupied molecular orbitals of $[\{Re(O)Br_2(3,5\text{-}Me_2pzH)_2\}_2(\mu\text{-}O)]$ with the largest contributions of d rhenium orbitals.

Among the occupied MOs of $[\{Re(O)Br_2(3,5\text{-}Me_2pzH)_2\}_2(\mu\text{-}O)]$, the largest numbers constitute orbitals of the pyrazole rings which are not relevant for the discussion of metal–oxo bonding. The nature bond of the O=Re–O–Re=O core was discussed for $[\{Re(O)Br_2(NH_3)_2\}_2(\mu\text{-}O)]$. Two bonding and one nonbonding σ-type MOs of the linear O=Re–O–Re=O core of $[\{Re(O)Br_2(NH_3)_2\}_2(\mu\text{-}O)]$ are depicted in Fig. 10.

The $d_{xz}$ and $d_{yz}$ orbitals of both rhenium ions interact with the filled $p_x$ and $p_y$ orbitals of the terminal and bridging oxo ligands to give four π-bonding, two π-nonbonding and four π-antibonding molecular orbitals. Fig. 11 presents the qualitative molecular orbital scheme for the π-bond system of dinuclear rhenium complexes with the linear O=Re–O–Re=O unit and views of the π-bonding, π-nonbonding and π-antibonding MO calculated for $[\{Re(O)Br_2(NH_3)_2\}_2(\mu\text{-}O)]$. In total, there are six delocalized bonding orbitals (two σ and four π) describing $Re_2O_3$ unit, which in the localized picture is equivalent to Re-$O_t$ double bonds and Re-$O_b$ single bonds.

### 2.3. Methods of synthesis

The dinuclear rhenium oxocomplexes with a linear O=Re–O–Re=O backbone were prepared by a variety of methods. The *cis*,*cis*-$[\{ReOCl_2(py)_2\}_2(\mu\text{-}O)]$ complex was obtained by Johnson et al. from the reaction of $[ReOCl_3(PPh_3)_2]$ with an excess of moist pyridine in benzene [46]. Refluxing of $[ReOCl_2(OMe)(py)_2]$ in toluene led to *trans*,*trans*-$[\{ReOCl_2(py)_2\}_2(\mu\text{-}O)]$ [21]. Blue crystals of *trans*,*trans*-$[\{ReOCl_2(1\text{-}Meim)_2\}_2(\mu\text{-}O)]$ appeared after several days upon recrystallization of $[ReCl_3(py)_2(PPh_3)]$ in acetone [20]. The orthorhombic polymorph of $[\{ReOCl_2(Me_2pzH)_2\}_2(\mu\text{-}O)]$ was prepared in the reaction of $NH_4ReO_4$ in ethanolic HCl with $K[HB(Me_2pz)_3]$. Such reaction conditions resulted in a breakup of the pyrazoylborate group to form 3,5-dimethylpyrazole ligands [13].

The $[\{ReOCl_2\}_2(\mu\text{-}O)(\mu\text{-dppm})_2]$ complex was isolated in the reaction of $[Re_2Cl_4(\mu\text{-dppm})_2]$ with molecular oxygen [41]:

$$[Re_2Cl_4(\mu - \text{dppm})_2] + O_2 \rightarrow [Re_2OCl_3(\mu - O)(\mu - Cl)(\mu - \text{dppm})_2]$$

$$[Re_2OCl_3(\mu - O)(\mu - Cl)(\mu - \text{dppm})_2] + \tfrac{1}{2}O_2 \rightarrow [\{ReOCl_2\}_2(\mu - O)(\mu - \text{dppm})_2]$$

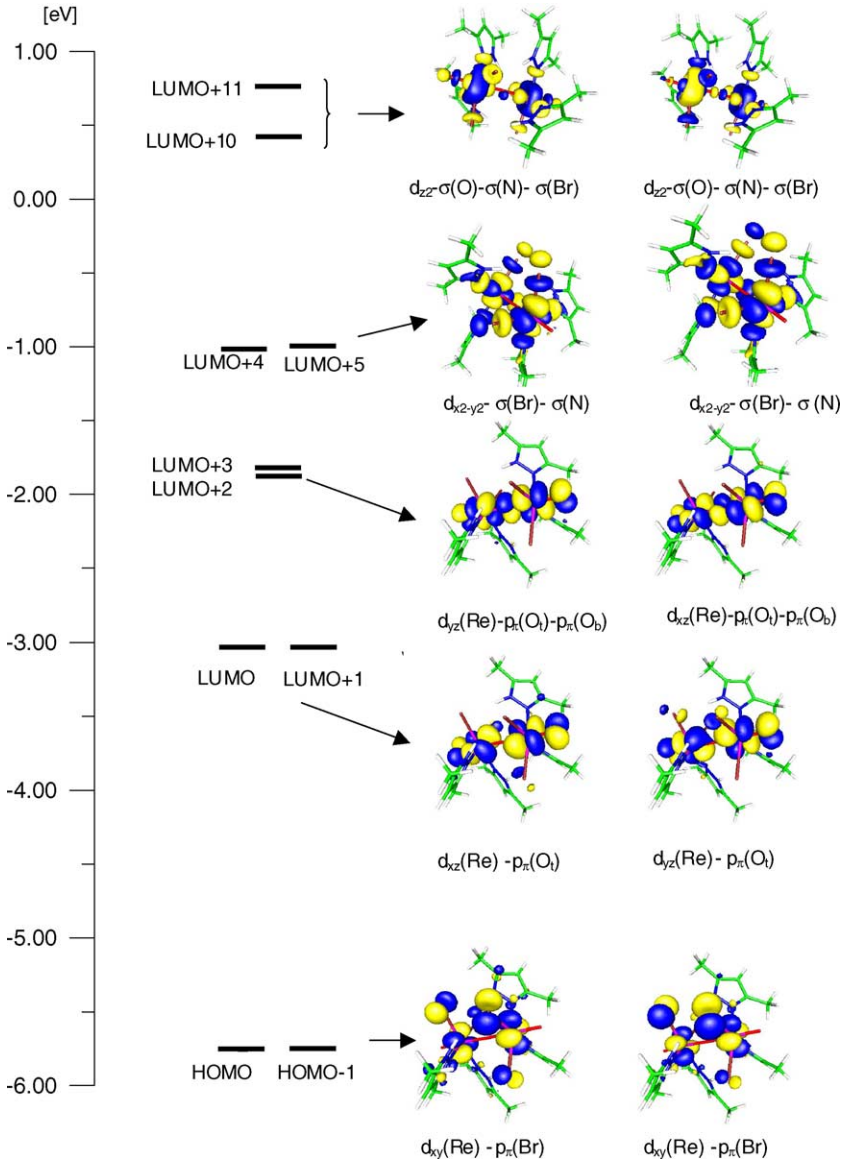


Fig. 9. The energy, character and contours of the occupied and unoccupied molecular orbitals of $[\{Re(O)Br_2(3,5\text{-}Me_2pzH)_2\}_2(\mu\text{-}O)]$ with the largest contributions of the d rhenium orbitals. The *z* axis goes along O=Re—O—Re=O linkage, *x* and *y* axes go through the Br—Re—$N_{pz}$ bonds.

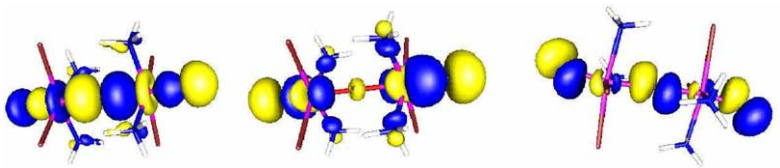

Fig. 10. The σ-bonding and σ-nonbonding molecular orbitals of $[\{Re(O)Br_2(NH_3)_2\}_2(\mu\text{-}O)]$.

The common way of the $[Re_2O_3X_4L_4]$ preparation seems to be treatment of $[ReOCl_3(Me_2S)(OPPh_3)]$ or $[ReOX_3(AsPh_3)(OAsPh_3)]$ (X=Cl, Br) with the L ligand. In the case of $[ReOCl_3(Me_2S)(OPPh_3)]$, dimerization can be performed in a stepwise manner. Treatment of $[ReOCl_3(Me_2S)(OPPh_3)]$ with 1 equiv. of $L_1$ leads to substitution of $Me_2S$ and formation of $[ReOCl_3(L_1)(OPPh_3)]$ which can easily react with other *N*-heterocyclic molecules (Scheme 4). The *rac*-$[\{ReOCl_2(Me_3Bzm)(py)\}_2(\mu\text{-}O)]$ and *meso*-$[\{ReOCl_2(Me_3Bzm)(3,4\text{-lut})\}_2(\mu\text{-}O)]$ complexes were prepared in this way [17]. $[ReOCl_3(OAsPh_3)(pzH)]$ and $[ReOBr_3(OAsPh_3)(pzH)]$ were also isolated, so a stepwise dimerization could be predicted for $[ReOX_3(AsPh_3)(OAsPh_3)]$ (X=Cl, Br) [47].

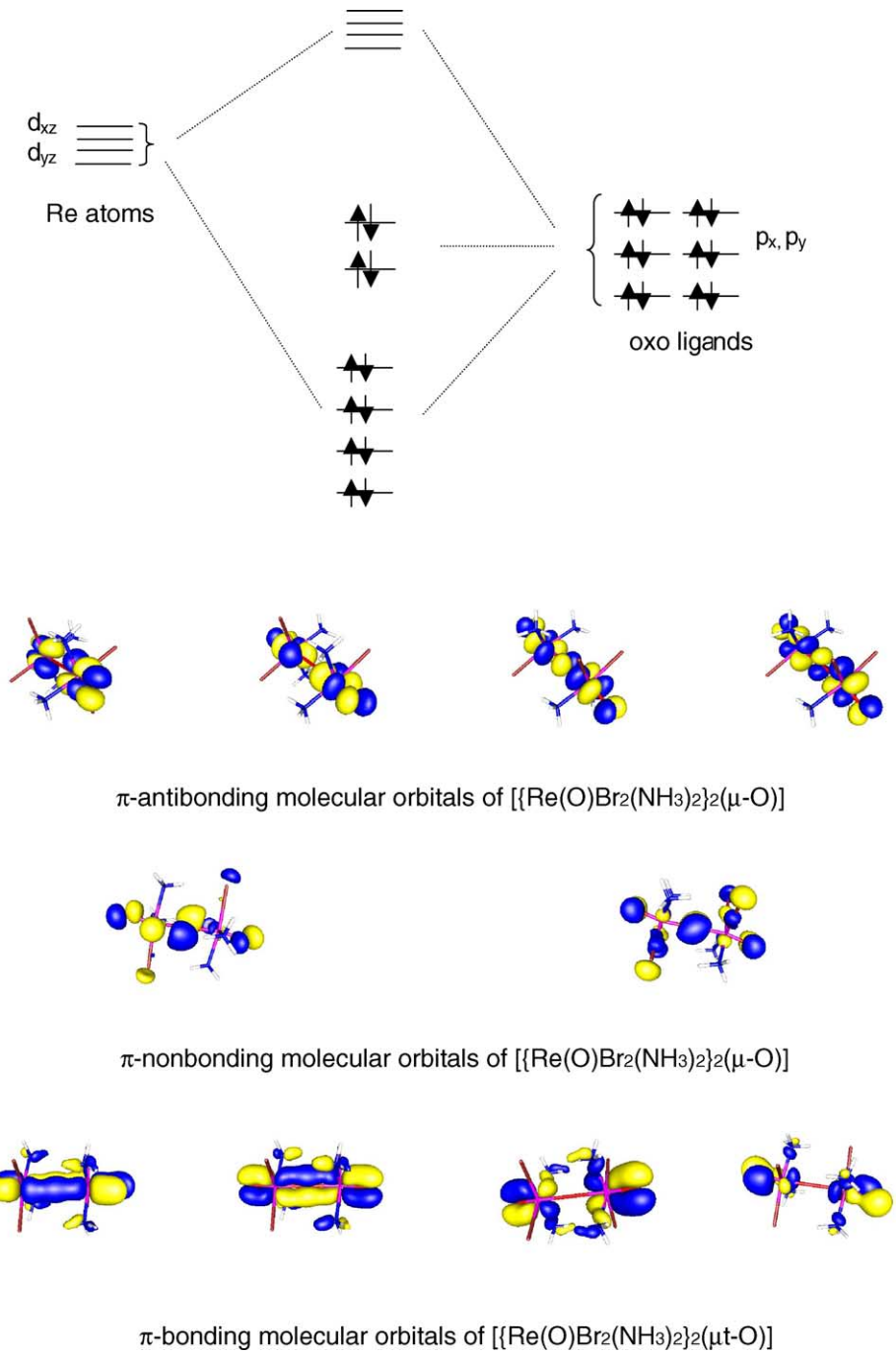


Fig. 11. The molecular orbital scheme for the π-bond system of dimers with a linear O=Re—O—Re=O unit and views of the π-bonding, π-nonbonding and π-antibonding MO calculated for $[\{Re(O)Br_2(NH_3)_2\}_2(\mu\text{-}O)]$.

Most of $[\{ReOX_2(L–L)\}_2(\mu\text{-}O)]$ and $[\{ReO(L_4)\}_2(\mu\text{-}O)]$ complexes was synthesized by the hydrolysis reactions of the corresponding mononuclear oxocomplexes $[ReOX_3(L–L)]$ or $[ReOX(L_4)]$, or in the reactions of *trans*-$[ReOX_3(PPh_3)_2]$ with an excess of the ligand in a system that was open to the atmosphere.

The factors determining the formation of the $Re_2O_3^{4+}$ complexes have not been formalised. Water seems to be the source of the bridging oxo group and the formation of intermediate hydroxo-species is crucial (Scheme 4). However, no intermediates have been isolated in the syntheses mentioned above.

### 2.4. IR spectroscopy

The IR spectra of dinuclear rhenium complexes with a linear O=Re–O–Re=O backbone show a sharp band in the range 900–1000 $cm^{-1}$ assignable to the symmetric Re=O stretch

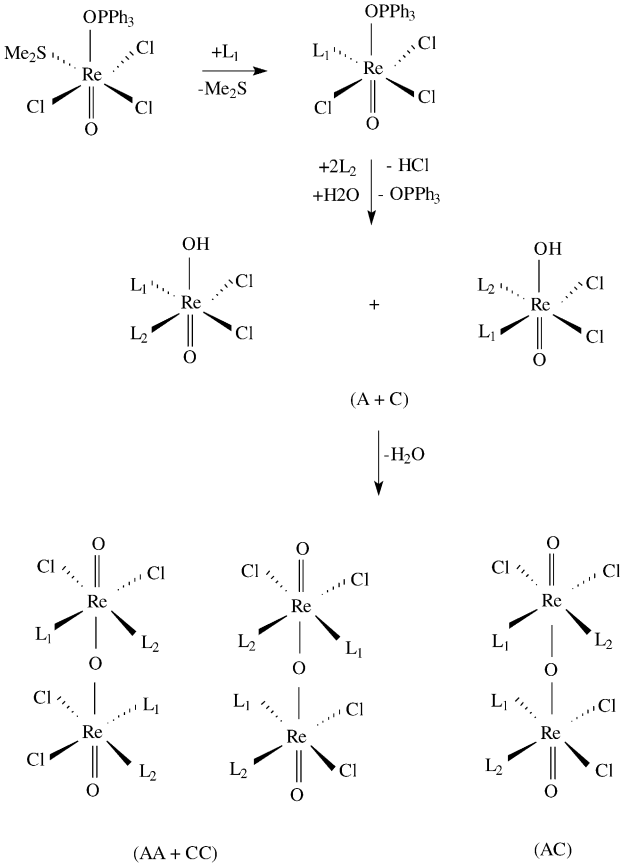


Scheme 4.

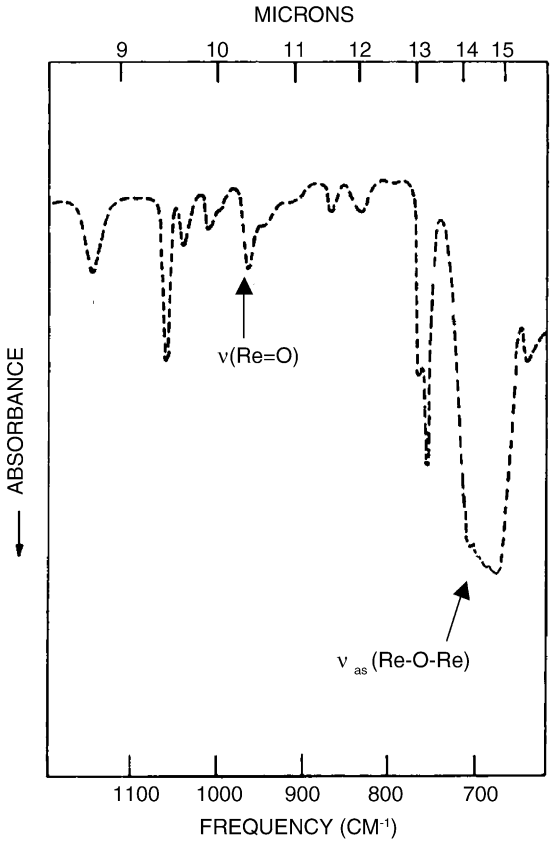


Fig. 12. The IR spectrum of the *cis*,*cis*-[{$ReOCl_2(py)_2$}$_2$(μ-O)] complex [49].

and a strong band in the range 720–630 $cm^{-1}$ attributed to the antisymmetric Re–O–Re stretching mode. In the case of dinuclear rhenium complexes with *N*-heterocyclic aromatic molecules in a coordination sphere, the $\nu_{as}$(Re–O–Re) stretching mode overlaps with the aromatic ring out-of-plane deformation vibrations to give a strong multicomponent band. Fig. 12 present the infrared spectrum (1200–650 $cm^{-1}$) of the *cis*,*cis*-[{$ReOCl_2(py)_2$}$_2$(μ-O)] complex [49].

The positions of the $\nu$(Re=O) and $\nu_{as}$(Re–O–Re) bands for rhenium complexes with a linear O=Re–O–Re=O backbone are shown in Table 5. The infrared spectroscopy seems to be a good probe to estimate the electron density at the rhenium atom and consequently the rhenium-oxygen bond order in these complexes. For some of these compounds significant differences are found in the $\nu$(Re=O) and $\nu_{as}$(Re–O–Re) stretching frequencies, although no clear difference in the bond lengths is noticed. Generally, the frequency of the $\nu_{as}$(Re–O–Re) stretching band decreases when the dentacity of ligands increases. A similar, but not so clear, trend is observed for $\nu$(Re=O) frequency. The antisymmetric $\nu_{as}$(Re–O–Re) stretching mode of the dinuclear rhenium complexes containing only bridging oxo ligand occurs at much higher energy; for $[(ReCl_5)_2(\mu\text{-}O)]^{4-}$ in the range 850–855 $cm^{-1}$ [50]. The reduction in the frequency of $\nu_{as}$(Re–O–Re) stretching mode in the complexes with a O=Re–O–Re=O framework is a consequence of the electron-withdrawing effect of the terminal Re=O group causing a relative weakening of the bridging Re–O bonds.

In comparison with monomeric compounds, the intensities of $\nu$(Re=O) stretching bands in dinuclear rhenium complexes with a linear O=Re–O–Re=O backbone are lower.

### 2.5. UV–vis spectroscopy

Table 6 presents the positions and molar absorptivity of the electronic bands for the dinuclear rhenium(V) complexes with a linear O=Re–O–Re=O backbone.

The UV–vis spectrum of [{$Re(O)Br_2$(3,5-$Me_2$pzH)$_2$}$_2$(μ-O)] was discussed basing on the electronic transitions calculated using the time-dependent DFT method [45]. The following assignments of the experimental absorption bands of [{$Re(O)Br_2$(3,5-$Me_2$pzH)$_2$}$_2$(μ-O)] was made based on the results of the TDDFT calculations. The longest wavelength experimental band of [{$Re(O)Br_2$(3,5-$Me_2$pzH)$_2$}$_2$(μ-O)] at 694.4 nm (Table 6) has d → d character. The band at 427.0 nm corresponds to the calculated transitions of π(Br) →d and π(pzH) →d character. The absorption band at 300.3 nm has also LMCT character and results from the transitions of π(O)/σ(Br) →d and π(Br) →d origin. The band at 255.8 nm is assigned to the calculated transitions of MLCT (d → π*(pzH)), and the band at 218.0 nm results from LMCT ($n_N$ →d)

Table 5
The position of $\nu$(Re=O) and $\nu_{as}$(Re—O—Re) for complexes with a linear O=Re—O—Re=O backbone

| Complex | $\nu$(Re=O) [$cm^{-1}$] | $\nu_{as}$(Re—O—Re) [$cm^{-1}$] | Ref. |
|---|---|---|---|
| $[\{ReOX_2L_2\}_2(\mu\text{-}O)]$ | | | |
| *cis,cis*-$[\{ReOCl_2(py)_2\}_2(\mu\text{-}O)]$ | 675 | 680 | [21] |
| $[\{ReOCl_2(Me_2pzH)\}_2(\mu\text{-}O)]\cdot Me_2CO$ | 972 | 704 | [13] |
| $[\{ReOCl_2(Me_2pzH)\}_2(\mu\text{-}O)]$ | 970 | 681 | [14] |
| $[\{ReOBr_2(Me_2pzH)\}_2(\mu\text{-}O)]$ | 969 | 682 | [14] |
| *rac*-$[\{ReOCl_2(Me_3Bzm)(py)\}_2(\mu\text{-}O)]$ | 969 | 687 | [17] |
| *rac*-$[\{ReOCl_2(Me_3Bzm)(3,5\text{-}lut)\}_2(\mu\text{-}O)]$ | 970 | 688 | [17] |
| *meso*-$[\{ReOCl_2(Me_3Bzm)(3,4\text{-}lut)\}_2(\mu\text{-}O)]$ | 968 | 690 | [17] |
| $[\{ReOCl_2(pyz)\}_2(\mu\text{-}O)]$ | 975 | 705 and 685 | [15] |
| $[\{ReOCl_2(pym)\}_2(\mu\text{-}O)]$ | 976 | 707 and 678 | [15] |
| *trans,trans*-$[\{ReOCl_2(py)_2\}_2(\mu\text{-}O)]$ | 980 | 675 | [21] |
| $[\{ReOX_2(L–L)\}_2(\mu\text{-}O)]$ | | | |
| $[\{ReOCl_2(eami)\}_2(\mu\text{-}O)]$ | 958 | 716 | [21] |
| $[\{ReOCl_2(etmi)\}_2(\mu\text{-}O)]$ | 974 | 694 | [21] |
| $[\{ReOCl_2(mami)\}_2(\mu\text{-}O)]$ | 937 | 719 | [21] |
| $[\{ReOCl_2(biimH_2)\}_2(\mu\text{-}O)]$ | 980 | 700-740 (br, vs) | [25] |
| $[\{ReOCl_2(R(CH_2)_2\ S(CH_2)_2S(CH_2)_2R')\}_2(\mu\text{-}O)]$ R,R′=H; R,R′=Et, R=S-Bu, R′=H; R=OEt, R′=H; R,R′= Et | 900–1000 | 650–700 | [24] |
| $[\{ReO(L_4)\}_2(\mu\text{-}O)]$ | | | |
| $[\{ReO(SCH_2CH_2NHCH_2CH_2SEt)_2\}_2(\mu\text{-}O)]$ | 928 | 660 | [28] |
| $[\{ReO(Me_2pymS)_2\}_2(\mu\text{-}O)]$ | 900 (m) | 709 (vs) | [29] |
| $[ReO(acac)\{\eta^2\text{-}B(pz)_4\}]_2(\mu\text{-}O)$ | 970 | 720 | [30] |
| $[\{ReO(dioxo\text{-}tetH_4)\}_2(\mu\text{-}O)]\cdot 4H_2O$ | 950 and 956 | 658 (br, s) | [35] |
| $[\{ReO\{N,N'\text{-}bis(2\text{-hydroxybenzyl})\text{-}1,3\text{-diaminopropane}\}_2]\ (\mu\text{-}O)$ | 951 | 692, 635 | [37] |
| $[\{ReO\{N,N'\text{-}bis(2\text{-hydroxybenzyl})\text{-}1,3\text{-diaminobutane}\}_2]\ (\mu\text{-}O)$ | 947 | 688, 632 | [37] |
| $[\{ReO(sal_2en)\}_2(\mu\text{-}O)]$ | 965 | 690 | [48] |
| $[\{ReO(sal_2phen)\}_2(\mu\text{-}O)]$ | 962 | 700 | [48] |
| $[\{ReO(acac_2en)\}_2(\mu\text{-}O)]$ | 975 | 720 | [48] |
| Others | | | |
| $[\{ReO(SCH_2CH_2NHCH_2CH_2SEt)(SR\}_2(\mu$ | | | [28] |
| R = $C_6H_5$ | 931 | 660 | |
| R = *p* | 933 | 671 | |
| R = *p* | 935 | 672 | |
| R = $C_6H_5CH_2$ | 932 | 669 | |

transitions and the $\pi\rightarrow\pi^*$ excitations in the pyrazole ligands. Due to similarity in positions of the experimental absorption bands for $[\{Re(O)Br_2(3,5\text{-}Me_2pzH)_2\}_2(\mu\text{-}O)]$ and $[\{Re(O)Cl_2(3,5\text{-}Me_2pzH)_2\}_2(\mu\text{-}O)]$, the assignments for chloro complex is analogous.

The longest wave experimental bands of *rac*-$[\{ReOCl_2(Me_3Bzm)(py)\}_2(\mu\text{-}O)]$, *rac*-$[\{ReOCl_2(Me_3Bzm)(3,5\text{-lut})\}_2(\mu\text{-}O)]$ and *meso*-$[\{ReOCl_2(Me_3Bzm)(3,5\text{-lut})\}_2(\mu\text{-}O)]$ are of low intensity and they probably arise from d $\rightarrow$d transitions. The increase in the intensity of the lowest energy absorption band observed for $[\{ReOCl_2(pyz)\}_2(\mu\text{-}O)]$, $[\{ReOCl_2(pym)\}_2(\mu\text{-}O)]$ and the complexes with bidentate ligands, indicates the participation of ligand-to-metal transitions. The absorption bands in the range 450–300 nm have LMCT character, mainly of $\pi$(O) $\rightarrow$d and $\pi$(hal) $\rightarrow$d origin.

### 2.6. NMR spectroscopy

Alessio and co-workers investigated the solution conformations of $[\{ReOCl_2(3,5\text{-lut})_2\}_2(\mu\text{-}O)]$, $[\{ReOCl_2(Me_3Bzm)_2\}_2(\mu\text{-}O)]$, *rac*-$[\{ReOCl_2(Me_3Bzm)(py)\}_2(\mu\text{-}O)]$ and *meso*-$[\{ReOCl_2(Me_3Bzm)(3,4\text{-lut})\}_2(\mu\text{-}O)]$ using 2D exchange nuclear Overhauser effect spectroscopy (NOESY/EXSY) [16,17,51]. The dimers were found to have a complicated dynamic behaviour in solution that involves (i) rotation about the Re—O—Re bond system, and (ii) rotation about the Re–N bonds. The rotation about the Re–O–Re bond system exchanges the stacking ligands with the terminal ones in a pairwise fashion and, when it is fast on the NMR time scale, involves the averaging of their resonances. The split of the corresponding H-signals is observed at much lower temperatures, when the rotation reaches the slow limit.

The restriction of rotation at room temperature is observed in the case of $[\{Re(O)Cl_2(3,5\text{-}Me_2pzH)_2\}_2(\mu\text{-}O)]$. The $^1H$ NMR spectrum of $[\{Re(O)Cl_2(3,5\text{-}Me_2pzH)_2\}_2(\mu\text{-}O)]$ recorded at 20 °C exhibits two sets of signals for each proton of coordinated 3,5-dimethylpyrazole molecules and considerable broadening of peaks is observed in the spectra of $[\{Re(O)Cl_2(3,5\text{-}Me_2pzH)_2\}_2(\mu\text{-}O)]$ at higher temperatures [14].

Table 6
The positions and molar absorptivity of the electronic bands for the dinuclear rhenium complexes with a linear O=Re─O─Re=O backbone

| Complex | Band position $cm^{-1}$] (molar absorptivity) ($dm^3\ mol^{-1}\ cm^{-1}$) | Transition assignments | Ref. |
|---|---|---|---|
| [{$ReOX_2L_2$}$_2$(μ-O)] | | | |
| [{$Re(O)Br_2$(3,5-$Me_2$pzH)$_2$}$_2$(μ-O)] | 694.4 (390) | d → d | [14,45] |
| | 427.0 (320) | π(Br) → d; π(pzH) → d | |
| | 300.3 (10230) | π(O)/σ(Br) → d; π(Br) → d | |
| | 255.8 (34650) | d → π*(pzH) | |
| | 218.0 (49670) | π(pzH) → π*(pzH) | |
| [{$Re(O)Cl_2$(3,5-$Me_2$pzH)$_2$}$_2$(μ-O)] | 693.5 (315) | d → d | [14,45] |
| | 388.8 (210) | π(Cl) → d; π(pzH) → d | |
| | 300.0 (14750) | π(O)/σ(Br) → d; π(Cl) → d | |
| | 249.0 (34730) | d → π*(pzH) | |
| | 222.4 (51360) | π(pzH) → π*(pzH) | |
| [{$ReOCl_2$($Me_2$pzH)}$_2$(μ-O)]·$Me_2CO$ | 681 (360) | d → d | [13,45] |
| | 329(2900) | π(O) → d; π(Cl) → d; π(pzH) → d | |
| *rac*-[{$ReOCl_2$($Me_3$Bzm)(py)}$_2$(μ-O)] | 677 (br, 350) | d → d | [17,45] |
| *rac*-[{$ReOCl_2$($Me_3$Bzm)(3,4-lut)}$_2$(μ-O)] | 680 (br, 360) | d → d | [17,45] |
| *meso*-[{$ReOCl_2$($Me_3$Bzm)(3,4-lut)}$_2$(μ-O)] | 686 (br, 430) | d → d | [17,45] |
| [{$ReOCl_2$(pyz)}$_2$(μ-O)] | 660 (1850) | d → d, π(Cl) → d | [15,45] |
| | 480 (3550) | π(Cl) → d; π(pyz) → d | |
| | 455 (3650) | π(Cl) → d; π(pyz) → d | |
| | 385 (5450) | π(O) → d; π(Cl) → d; π(pyz) → d | |
| [{$ReOCl_2$(pym)}$_2$(μ-O)] | 665 (br) | d → d, π(Cl) → d | [15,45] |
| | 355 (sh) | π(O) → d; π(Cl) → d; π(pym) → d | |
| [{$ReOX_2$(L–L)}$_2$(μ-O)] | | | |
| [{$ReOCl_2$(eami)}$_2$(μ-O)] | 649 (2400) | d → d, π(Cl) → d | [21,45] |
| | 409 (3400) | π(O) → d; π(Cl) → d; π(eami) → d | |
| [{$ReOCl_2$(etmi)}$_2$(μ-O)] | 648 (300) | d → d, π(Cl) → d | [21,45] |
| | 352 (2150) | π(O)→d; π(Cl) → d; π(etmi) → d | |
| [{$ReOCl_2$(mami)}$_2$(μ-O)] | 655 (1900) | d → d, π(Cl) → d | [21,45] |
| | 397 (4200) | π(O) → d; π(Cl) →d ; π(mami) → d | |
| [{$ReOCl_2$($Bu^nSCH_2CH_2SBu^n$)}$_2$(μ-O)] | 618 (500) | d → d | [24,45] |
| | 308 (19950) | π(O) → d; π(Cl) → d; π(L) → d | |
| [{$ReO(L_4)$}$_2$(μ-O)] | | | |
| [{$ReO$($Me_2$pymS)$_2$}$_2$(μ-O)] | 775 sh, 690, | d → d | [29,45] |
| | 642, 610 sh, | d → d | |
| | 574, | d → d | |
| | 550, 445 sh, | π(O) → d; π($Me_2$pymS) → d | |
| | 315 | π(O) → d; π($Me_2$pymS) → d | |
| | 250 | π($Me_2$pymS) → π*($Me_2$pymS) | |
| | 775 sh, 690, | d → d | |

## 3. Dinuclear complexes with a bent Re–O–Re unit

### 3.1. Structural properties

A bent Re–O–Re core was found in Re(V), Re(IV), Re(VI) and Re(VII) dinuclear complexes [14,25, 52–59]. The basal coordination sites of each Re(V) atom of [$Re_2O_3(L^2)_2(PMe_2Ph)_2$] are occupied by two deprotonated nitrogens of the ligand $L^2$ and the neutral nitrogen of the aminothiazole of a second molecule of ligand $L^2$. A molecule of $PR_3$ completes the basal coordination (Scheme 5B) [56]. Two metal centers of the other structurally characterised rhenium(V) dimers [14,25,52–55] are also in a pseudo-octahedral environment and they are linked through an oxo group and two bridging *N–N* bidentate ligands (Scheme 5A). The bend of the Re–O–Re unit in these complexes is a consequence of steric requirements of the bridging molecules.

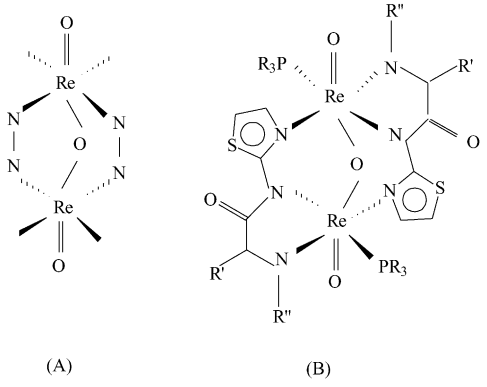


Scheme 5.

Table 7
The selected bond lengths [Å] and angles [°] for dinuclear rhenium complexes with a bent Re─O─Re unit

| Complex | Re─$O_t$ | Re─$O_b$ | $O_t$─Re─$O_b$ | Re─$O_b$─Re | Ref. |
|---|---|---|---|---|---|
| Re(V) | | | | | |
| $[\{ReOBr(3,5\text{-}Me_2pzH)\}_2(\mu\text{-}O)(\mu\text{-}3,5\text{-}Me_2pz)_2]$ | 1.687(6) | 1.909(5) | 168.4(2) | 122.7(3) | [14] |
| | 1.677(6) | 1.946(5) | 168.6(3) | 121.3(3) | |
| | 1.686(6) | 1.924(5) | 169.8(3) | | |
| | 1.677(6) | 1.943(5) | 168.1(3) | | |
| $[\{ReOCl(PPh_3)\}_2(\mu\text{-}O)(\mu\text{-}3,5\text{-}Me_2pz)_2]$ | 1.692(2) | 1.929(1) | 168.9(4) | 124.0(2) | [14] |
| $[\{Re(O)Cl(PPh_3)\}(\mu\text{-}O)(\mu\text{-}3,5\text{-}Me_2pz)_2\ \{Re(O)Cl(3,5\text{-}Me_2pzH)\}]$ | 1.692(8) | 1.931(7) | 168.9(4) | 123.3(4) | [14] |
| | 1.660(9) | 1.939(8) | 166.3(4) | | |
| $[\{Re(O)Br(PPh_3)\}(\mu\text{-}O)(\mu\text{-}3,5\text{-}Me_2pz)_2\ \{Re(O)Br(3,5\text{-}Me_2pzH)\}]$ | 1.688(7) | 1.915(6) | 170.2(3) | 123.5(3) | [14] |
| | 1.664(7) | 1.940(6) | 166.2(3) | | |
| $[\{Re(O)Cl(PPh_3)\}_2(\mu\text{-}O)(\mu\text{-}pz)_2]$ | 1.686(7) | 1.946(7) | 162.6(4) | 124.1(4) | [52] |
| | 1.690(8) | 1.941(7) | 161.5(3) | | |
| $[\{Re(O)Cl(PPh_3)\}_2(\mu\text{-}O)(\mu\text{-}pz\text{-}4\text{-}NO_2)_2]$ | 1.696(17) | 1.912(15) | 163.3(6) | 124.5(6) | [53] |
| | 1.713(14) | 1.969(14) | 163.9(6) | | |
| $[\{Re(O)Cl(PPh_3)\}_2(\mu\text{-}O)(\mu\text{-}C_6H_4N_3)_2]$ | 1.688(10) | 1.916(9) | 163.4(5) | 125.2(4) | [54] |
| | 1.691(10) | 1.951(8) | 163.2(4) | | |
| $[\{Re(O)Br(PPh_3)\}_2(\mu\text{-}O)(\mu\text{-}C_6H_4N_3)_2]$ | 1.671(6) | 1.924(5) | 162.7(3) | 126.0(3) | [54] |
| | 1.674(6) | 1.938(5) | 163.0(3) | | |
| $[\{ReO[H(F)B(pz)_2]\}_2(\mu\text{-}O)(\mu\text{-}pz)_2]$ | 1.654(12) | 1.925(11) | 166.2(7) | 124.2(7) | [55] |
| | 1.687(14) | 1.932(12) | 166.8(5) | | |
| $[\{ReO[\eta^2\text{-}B(pz)_4]\}_2(\mu\text{-}O)(\mu\text{-}pz)_2]$ | 1.680(6) | 1.930(5) | 164.6(2) | 125.4(3) | [30] |
| | 1.693(6) | 1.923(5) | 166.1(3) | | |
| $[Re_2O_3(L^2)_2(PMe_2Ph)_2]$ | 1.690(7) | 1.925(7) | 166.7(3) | 138.3(4) | [56] |
| | 1.684(7) | 1.897(7) | 165.7(3) | | |
| $[\{ReOCl_2\}_2(\mu\text{-}O)(\mu\text{-}biimMe_2)_2]$ | 1.685(5) | 1.894(5) | 168.2(2) | 162.6(3) | [25] |
| | 1.681(6) | 1.897(5) | 166.0(2) | | |
| Mean | 1.682 | 1.931 | | | |
| Re(VI) | | | | | |
| $[\{ReO(OMe)_2\}_2(\mu\text{-}O)(\mu\text{-}OMe)_2]$ | 1.690(11) | 1.917(13) | 99.4(6) | 83.8(5) | [58] |
| | 1.703(12) | 1.916(13) | 99.8(6) | | |
| $[\{ReO(Me)_2\}_2(\mu\text{-}O)(\mu\text{-}CH_2)]$ | 1.675 | 1.939 | 118.3 | 87.4 | [59] |
| | 1.626 | 1.902 | 114.2 | | |
| Re(VII) | | | | | |
| $[\{ReO(H_2O)(O_2)_2\}_2(\mu\text{-}O)]\cdot(diglyme)_2$ | 1.674(9) | 1.86(1) | 97.2(5) | 150.6(5) | [60] |
| | | 1.90(1) | 97.6(4) | | |

For all the complexes with the bridging pyrazoyl ligands, the Re–O–Re angle is near 120° (Table 7).

The bridging *N–N* ligands introduce some additional strain in the dimers. Consequently, the distortions from the ideal octahedron in the complexes with a bent Re–O–Re unit are considerable greater in comparison with those found in the complexes containing a linear O=Re–O–Re=O backbone.

A thermal ellipsoid plot of $[\{ReOCl_2\}_2(\mu\text{-}O)(\mu\text{-}biimMe_2)_2]$ is depicted in Fig. 13. The two imidiazole rings

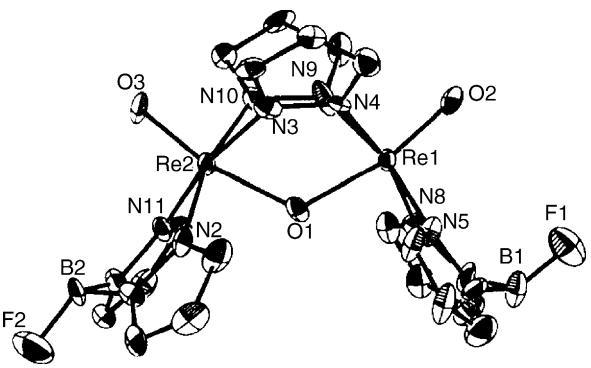


Fig. 13. Structure of $[\{ReO[H(F)Bpz_2]\}_2(\mu\text{-}O)(\mu\text{-}pz)_2]$ [55].

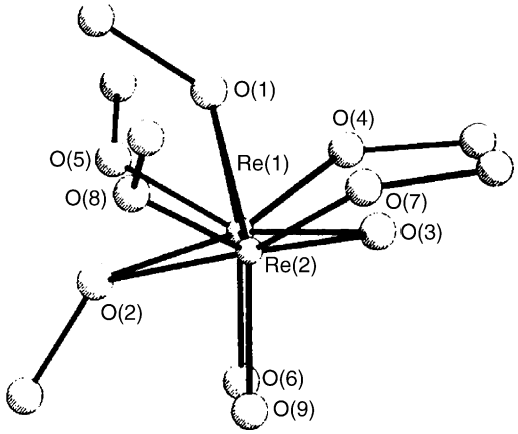


Fig. 14. Structure of $[\{ReO(OMe)_2\}_2(\mu\text{-}O)(\mu\text{-}OMe)_2]$ [58].

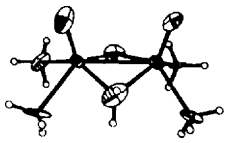

Fig. 15. Structure of [{ReO(Me)$_2$}$_2$(μ-O)(μ-CH$_2$)] [59].

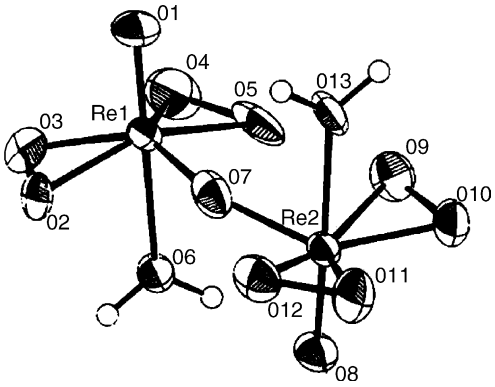


Fig. 16. Structure of [{ReO(H$_2$O)(O$_2$)$_2$}$_2$(μ-O)] [60].

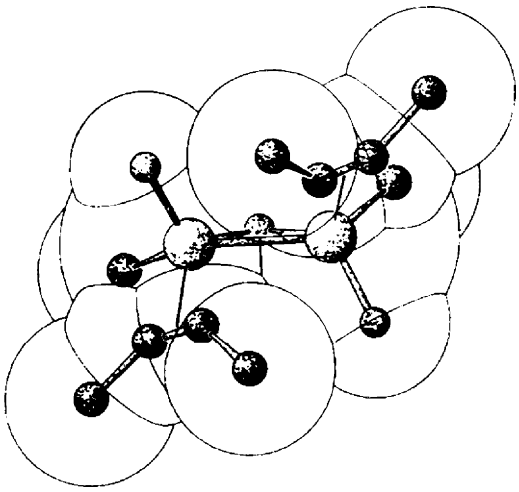

Fig. 17. Structure of [{ReO(Me)(η$^2$-MeC≡CMe)}$_2$(μ-O)] [57].

of the complex can interact by π stacking. The planes of these imidiazole rings are almost parallel and the distance between the ring centres is 3.3 Å [25]. The fluorine and hydrogen atoms of [H(F)Bpz$_2$] are disordered in the structure

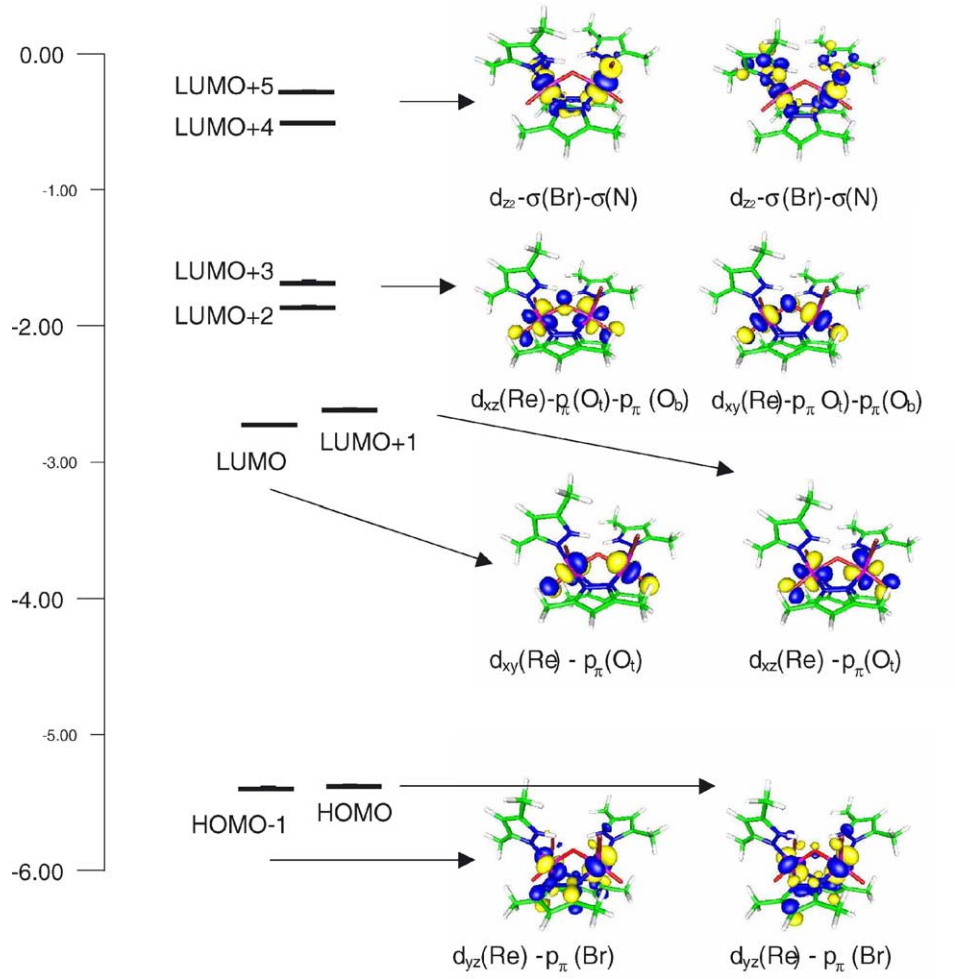


Fig. 18. The energy (eV), character and contours of the occupied and unoccupied molecular orbitals of [{Re(O)Br(3,5-Me$_2$pzH)}$_2$(μ-O)(μ-3,5-Me$_2$pz)$_2$] with the largest contributions of the d rhenium orbitals. The *x* and *z* axes go along O$_t$—Re—O$_b$ and Br—Re—N$_b$, respectively.

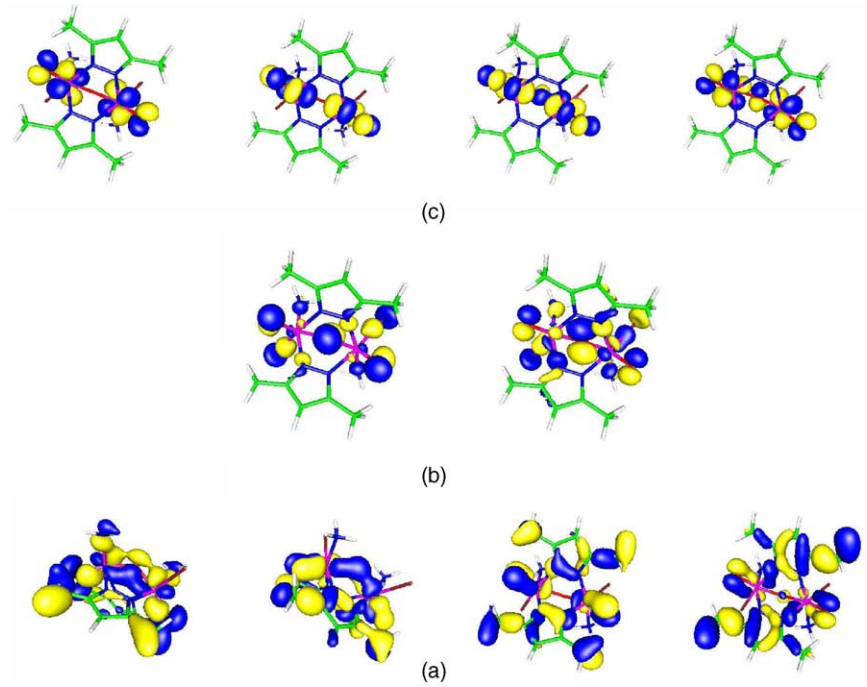


Fig. 19. The views of the π-bonding (a), π-nonbonding (b) and π-antibonding (c) MOs calculated for $[\{Re(O)Br(NH_3)\}_2(\mu\text{-}O)(\mu\text{-}3,5\text{-}Me_2pz)_2]$.

of $[\{ReO[H(F)Bpz_2]\}_2(\mu\text{-}O)(\mu\text{-}pz)_2]$, they are either *syn* or *anti* with respect to the nearby terminal oxo ligand [55].

The structure of $[\{ReO(OMe)_2\}_2(\mu\text{-}O)(\mu\text{-}OMe)_2]$ contains two rhenium atoms bridged by one oxo- and two methoxo-groups and has the overall geometry of a confacial bioctahedron with considerable distortion [58]. A perspective drawing of $[\{ReO(OMe)_2\}_2(\mu\text{-}O)(\mu\text{-}OMe)_2]$ is shown in Fig. 14.

Each rhenium centre of the $[\{ReO(Me)_2\}_2(\mu\text{-}O)(\mu\text{-}CH_2)]$ complex, presented in Fig. 15, has a square-pyramidal geometry with the terminal oxo ligand in apical position [59].

The acute angles at the bridging atoms of $[\{ReO(OMe)_2\}_2(\mu\text{-}O)(\mu\text{-}OMe)_2]$ and $[\{ReO(Me)_2\}_2(\mu\text{-}O)(\mu\text{-}CH_2)]$, and the short Re–Re distance (2.559 and 2.654 Å, respectively) are consistent with the presence of a Re–Re single bond, as required by the observed diamagnetism of the compound.

The rhenium atoms in $[\{ReO(H_2O)(O_2)_2\}_2(\mu\text{-}O)]\cdot(diglyme)_2$ are coordinated by seven oxygen atoms. If a peroxo ligands is considered as one structural unit, the coordination geometry can be described as a distorted trigonal bipyramid. The two $\eta^2$-peroxo groups and the bridging oxygen occupy equatorial positions, while the terminal oxo ligands and the water molecules are axial [60]. The solid-state structure of this peroxide complex is shown in Fig. 16.

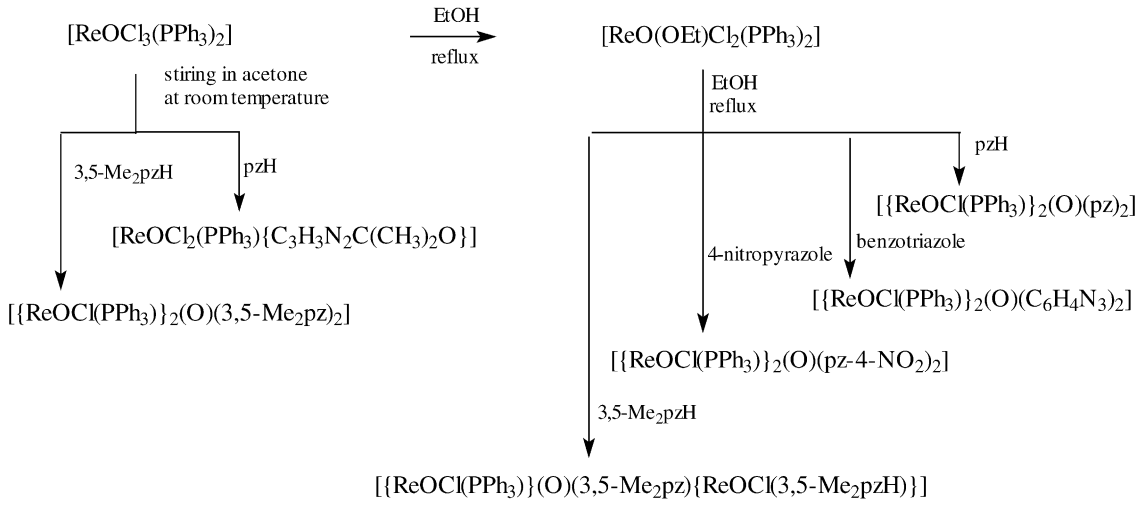


Scheme 6.

The [{ReO(Me)($\eta^2$-MeC≡CMe)}$_2$($\mu$-O)] complex has an equilateral $Re_2O$-triangular core geometry with the ligands O, $CH_3$, and butyne arranged in such way that $C_2$-symmetry results [57]. A perspective view of [{ReO(Me)($\eta^2$-MeC≡CMe)}$_2$($\mu$-O)] is presented in Fig. 17.

The Re–$O_t$ and Re–$O_b$ bond lengths of Re(V) dimers with a bent Re–O–Re unit are in the ranges of 1.660–1.713 and 1.884–1.969Å, respectively. The average Re–$O_t$ and Re–$O_b$ distances are equal 1.682 and 1.931Å, respectively. No clear difference is noticed in comparison with the Re–$O_t$ and Re–$O_b$ values found for the dirhenium complexes with a linear O=Re–O–Re=O backbone.

### 3.2. Electronic structure

The electronic structures of [{Re(O)Br(3,5-$Me_2$pzH)}$_2$($\mu$-O)($\mu$-3,5-$Me_2$pz)$_2$] and model compound — [{Re(O)Br($NH_3$)}$_2$($\mu$-O)($\mu$-3,5-$Me_2$pz)$_2$] were examined using the density functional theory (DFT) [45]. The qualitative molecular orbitals scheme for [{Re(O)Br(3,5-$Me_2$pzH)}$_2$($\mu$-O)($\mu$-3,5-$Me_2$pz)$_2$] is almost the same as for [{Re(O)$Br_2$(3,5-$Me_2$pzH)$_2$}$_2$($\mu$-O)] with a linear O=Re–O–Re=O core. The rhenium atoms of [{Re(O)Br(3,5-$Me_2$pzH)}$_2$($\mu$-O)($\mu$-3,5-$Me_2$pz)$_2$] possess $d^2$ electronic configuration. Two highest occuppied MOs of [{Re(O)Br(3,5-$Me_2$pzH)}$_2$($\mu$-O)($\mu$-3,5-$Me_2$pz)$_2$] are $d_{yz}$ with an antibonding contributions from $p_\pi$ bromine orbitals. The remaining d-type orbitals of rhenium are found among unoccuppied MOs, some of them bear antibonding character towards the oxygen atoms. Fig. 18 presents the energy and contours of the occupied and unoccupied molecular orbitals of [{Re(O)Br(3,5-$Me_2$pzH)}$_2$($\mu$-O)($\mu$-3,5-$Me_2$pz)$_2$] with the largest contributions of d rhenium orbitals. The energy of $d_{x2-y2}$ orbitals is much higher. The values of the HOMO-LUMO energy gap for complexes [{Re(O)$Br_2$(3,5-$Me_2$pzH)$_2$}$_2$($\mu$-O)] and [{Re(O)Br(3,5-$Me_2$pzH)}$_2$($\mu$-O)($\mu$-3,5-$Me_2$pz)$_2$] are equal to 2.71 and 2.64 eV, respectively. It is higher for the complex with a linear O=Re–O–Re=O unit, which indicates the higher stability of the complex and explain the formation of [{Re(O)Br(3,5-$Me_2$pzH)}$_2$($\mu$-O)($\mu$-3,5-$Me_2$pz)$_2$] in such low yield [14]. Fig. 19 presents the views of the $\pi$-bonding, $\pi$-nonbonding and $\pi$-antibonding MO calculated for [{Re(O)Br($NH_3$)}$_2$($\mu$-O)($\mu$-3,5-$Me_2$pz)$_2$].

### 3.3. Methods of synthesis

Pyrazole, benzotriazole and their derivatives can coordinate in a monodentate way or act as bridging ligands [61,62]. The studies [14,52–54] show that these ligands easily react with [$ReOX_3(PPh_3)_2$] to give dimers with a bent Re–O–Re unit and two bridging heterocyclic molecules. Treatment of [$ReOX_3(PPh_3)_2$] with 3,5-$Me_2$pzH in acetone at room temperature leads to the isolation of the symmetrically substituted dinuclear rhenium complexes [{Re(O)X($PPh_3$)}$_2$($\mu$-O)($\mu$-3,5-$Me_2$pz)$_2$], but refluxing of [ReO(OEt)$X_2(PPh_3)_2$] complexes with 3,5-$Me_2$pzH in ethanol gives the unsymmetrically substituted dinuclear rhenium [{Re(O)X($PPh_3$)}($\mu$-O)($\mu$-3,5-$Me_2$pz)$_2${Re(O)X(3,5-

Table 8
The position of $\nu$(Re=O) and $\nu_{as}$(Re—O—Re) for complexes with a bent Re—O—Re unit

| Complex | $\nu$(Re=O) [$cm^{-1}$] | $\nu_{as}$(Re—O—Re) [$cm^{-1}$] | Ref. |
|---|---|---|---|
| Re(V) | | | |
| [{ReOBr(3,5-$Me_2$pzH)}$_2$($\mu$-O)($\mu$-3,5-$Me_2$pz)$_2$] | 966, 962 | 671 (s), 651 (s), 634 (vs) | [14] |
| [{Re(O)Cl($PPh_3$)}$_2$($\mu$-O)($\mu$-3,5-$Me_2$pz)$_2$] | 957 | 679 (s), 621 (w) | [14] |
| [{Re(O)Cl($PPh_3$)}($\mu$-O)($\mu$-3,5$Me_2$pz)$_2$ {Re(O)Cl(3,5-$Me_2$pzH)}] | 963, 959 | 669 (s), 637 (vs) | [14] |
| [{Re(O)Br($PPh_3$)}($\mu$-O)($\mu$-3,5$Me_2$pz)$_2$ {Re(O)Br(3,5-$Me_2$pzH)}] | 963 (s), 959 (s) | 667 (s), 633 (vs) | [14] |
| [{Re(O)Cl($PPh_3$)}$_2$($\mu$-O)($\mu$-pz)$_2$] | 958 | 670 (w), 623 (vs), 616 (sh) | [52] |
| [{Re(O)Br($PPh_3$)}$_2$($\mu$-O)($\mu$-pz)$_2$] | 959 | 667 (w), 630 (vs), 614 (sh) | [52] |
| [{Re(O)Cl($PPh_3$)}$_2$($\mu$-O)($\mu$-pz-4-$NO_2$)$_2$] | 972 | 693 (s), 629 (s) | [53] |
| [{Re(O)Cl($PPh_3$)}$_2$($\mu$-O)($\mu$-$C_6H_4N_3$)$_2$] | 969 | 636 (vs), 615 (sh) | [54] |
| [{Re(O)Br($PPh_3$)}$_2$($\mu$-O)($\mu$-$C_6H_4N_3$)$_2$] | 969 | 629 (vs), 615 (sh) | [54] |
| [{ReO[H(F)Bpz$_2$]}$_2$($\mu$-O)($\mu$-pz)$_2$] | 965 | 688 (w), 675 (w), 642 (m) | [55] |
| [{ReO[$\eta^2$-B(pz)$_4$]}$_2$($\mu$-O)($\mu$-pz)$_2$] | 967 | 637 | [30] |
| [{ReO[$\eta^2$-B(pz)$_4$]}$_2$($\mu$-O)($\mu$-3,5-$Me_2$pz)$_2$] | 968 | 639 | [30] |
| [$Re_2O_3(L^1)_2(PMe_2Ph)_2$] | 945, 912 | 671 | [56] |
| [$Re_2O_3(L^2)_2(PMe_2Ph)_2$] | 910 | 671 | |
| [$Re_2O_3(L^3)_2(PMe_2Ph)_2$] | 934, 910 | 670 | |
| [$Re_2O_3(L^2)_2(PMePh_2)_2$] | 937, 894 | 695 | |
| Re(IV) | | | |
| [{ReO(Me)($\eta^2$-EtC≡CEt)}$_2$($\mu$-O)] | 977, 971 | | [57] |
| Re(VI) | | | |
| [{ReO(OMe)$_2$}$_2$($\mu$-O)($\mu$-OMe)$_2$] | 986, 982 | | [58] |
| [{ReO(Me)$_2$}$_2$($\mu$-O)($\mu$-$CH_2$)] | 1014, 1001 | 748 | [59] |
| Re(VII) | | | |
| [{ReO($H_2O$)($O_2$)$_2$}$_2$($\mu$-O)]·(diglyme)$_2$ | 932 | | [60] |

Table 9
The positions and molar absorptivity of the electronic bands for the dinuclear rhenium complexes with a bent Re—O—Re core

| Complex | Band position [$cm^{-1}$] (molar absorptivity) [$dm^3\ mol^{-1}\ cm^{-1}$] | Transition assignments | Ref. |
|---|---|---|---|
| [{Re(O)Br(3,5-$Me_2$pzH)}$_2$(μ-O)(μ-3,5-$Me_2$pz)$_2$] | 690.6 (180) | d→d | [14,45] |
| | 300.0 (5700) | π(Br)/π(pz)→d | |
| | 274.4 (8200) | π(O)/π(Br)/π(pz)→d; d→π*(pz) | |
| | 232.0 (22850) | d→π*(pz) | |
| | 222.2 (13750) | π(pz)→π*(pz) | |
| [{Re(O)Cl($PPh_3$)}$_2$(μ-O)(μ-3,5-$Me_2$pz)$_2$] | 656.6 (115) | d→d | [14,45] |
| | 332.0 (2150) | π(Cl)/π(pz)/π(Ph)→d; | |
| | 267.0 (8965) | π(O)/π(Cl)π(pz)/π(Ph)→d; d→π*(pz)/(Ph) | |
| | 232.0 (39410) | d→π*(pz)/π*(Ph) | |
| | 221.0 (22750) | π(pz)→π*(pz); π(Ph)→π*(Ph) | |
| [{Re(O)Br($PPh_3$)}$_2$(μ-O)(μ-3,5-$Me_2$pz)$_2$] | 646.8 (105) | d→d | [14,45] |
| | 379.5 (1500) | π(O)/π(Br)/π(pz)→d | |
| | 250.5 (25550) | d→π*(pz)/π*(Ph) | |
| | 220.0 (53515) | π(pz)→π*(pz); π(Ph)→π*(Ph) | |
| [{Re(O)Cl($PPh_3$)}(μ | 691.6 (230) | d→d | [14,45] |
| {Re(O)Cl(3,5 | 265.6 (15000) | π(O)/π(Br)/π(pz)→d; d→π*(pz)/(Ph) | |
| | 232.8 (30650) | d→π*(pz)/π*(Ph) | |
| | 220.4 (29550) | π(pz)→π*(pz); π(Ph)→π*(Ph) | |
| [{Re(O)Br($PPh_3$)}(μ | 702.0 (285) | d→d | [14,45] |
| {Re(O)Br(3,5 | 265.6 (14600) | π(O)/π(Br)/π(pz)→d; d→π*(pz)/(Ph) | |
| | 231.5 (37830) | d→π*(pz)/π*(Ph) | |
| | 220.0 (30250) | π(pz)→π*(pz), π(Ph)→π*(Ph) | |
| [{Re(O)Cl($PPh_3$)}$_2$(μ-O)(μ-pz)$_2$] | 652.3 (315) | d→d | [52,45] |
| | 400.2 (850) | d→d | |
| | 331.8 (6430) | π(Cl)/π(pz)/π(Ph)→d | |
| | 265.0 (12500) | π(O)/π(Cl)π(pz)/π(Ph)→d; d→π*(pz)/(Ph) | |
| | 232.6 (57120) | d→π*(pz)/π*(Ph) | |
| | 224.2 (30400) | π(pz)→π*(pz), π(Ph)→π*(Ph) | |
| [{Re(O)Br($PPh_3$)}$_2$(μ-O)(μ-pz)$_2$] | 656.6 (315) | d→d | [52,45] |
| | 418.1 (670) | d→d | |
| | 328.8 (8250) | π(Br)/π(pz)/π(Ph)→d | |
| | 269.0 (15250) | π(O)/π(Br)π(pz)/π(Ph)→d; d→π*(pz)/(Ph) | |
| | 249.8 (50970) | d→π*(pz)/π*(Ph) | |
| | 220.0 (30350) | π(pz)→π*(pz), π(Ph)→π*(Ph) | |
| [{Re(O)Cl($PPh_3$)}$_2$(μ-O)(μ-$C_6H_4N_3$)$_2$] | 621.9 (545) | d→d | [54,45] |
| | 420.0 (1050) | d→d; π(Cl)/π(bz)/π(Ph)→d | |
| | 340.1 (12460) | π(Cl)/π(bz)/π(Ph)→d | |
| | 303.0 (25000) | π(O)/π(Cl)π(bz)/π(Ph)→d; d→π*(bz)/(Ph) | |
| | 239.0 (48800) | d→π*(bz)/π*(Ph) | |
| | 228.1 (46600) | π(pz)→π*(pz), π(Ph)→π*(Ph) | |
| [{Re(O)Br($PPh_3$)}$_2$(μ-O)(μ-$C_6H_4N_3$)$_2$] | 654.9 (310) | d→d | [54,45] |
| | 410.0 (890) | d→d; π(Br)/π(bz)/π(Ph)→d | |
| | 331.5 (9060) | π(Br)/π(bz)/π(Ph)→d | |
| | 300.0 (11780) | π(O)/π(Br)π(bz)/π(Ph)→d; d→π*(bz)/(Ph) | |
| | 239.6 (44200) | d→π*(bz)/π*(Ph) | |
| | 225.0 (42750) | π(pz)→π*(pz), π(Ph)→π*(Ph) | |
| [{ReO[η$^2$-B(pz)$_4$]}$_2$(μ-O)(μ-pz)$_2$] | 583 | d→d | [30] |
| [{ReO[η$^2$-B(pz)$_4$]}$_2$(μ-O)(μ-3,5-$Me_2$pz)$_2$] | 617 | d→d | [30] |
| [{ReO($H_2O$)($O_2$)$_2$}$_2$(μ-O)] | 350 (1314) | π(O)→d | [60] |

$Me_2$pzH)}] complexes [14]. For benzotriazole and nitropyrazole, only the symmetrically substituted dinuclear rhenium [{Re(O)X($PPh_3$)}$_2$(μ-O)(μ-$C_6H_4N_3$)$_2$] and [{Re(O)Cl($PPh_3$)}$_2$(μ-O)(μ-pz-4-$NO_2$)$_2$] complexes have been isolated in the reactions of [$ReOX_3(PPh_3)_2$] with benzotriazole or nitropyrazole [53,54]. Refluxing of [$ReOX_3(PPh_3)_2$] complexes pzH in ethanol leads to [{Re(O)X($PPh_3$)}$_2$(μ-O)(μ-$N_2C_3H_3$)$_2$], but treatment of [$ReOX_3(PPh_3)_2$] with pzH in acetone at room temperature gives the mononuclear rhenium(V) complexes — [Re(O)$X_2$($PPh_3$)(η$^2$-$N_2C_6H_9$O-N,O)] (Scheme 6). In the second case, pyrazole firstly adds to acetone yielding $C_3H_3N_2C(CH_3)_2OH$ adduct, which reacts with the starting oxo complex [52]:

$$[ReOX_3(PPh_3)_2] + C_3H_3N_2C(CH_3)_2OH \rightarrow [ReOX_2\{\eta^2\text{-}O(CH_3)_2CN_2C_3H_3\}(PPh_3)] + HX + PPh_3$$

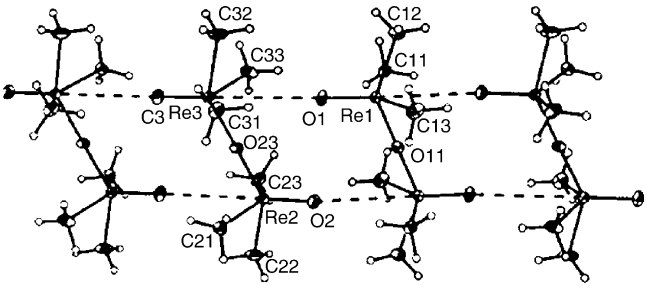


Fig. 20 Structure of. $[\{ReO(CH_3)_3\}_2(\mu\text{-}O)]$ [63].

Replacement of $[ReOX_3(PPh_3)_2]$ in the synthesis by $[ReOX_3(AsPh_3)(OAsPh_3)]$ or $[ReOCl_3(Me_2S)(OPPh_3)]$ complexes leads to the isolation of dimers with a linear O=Re–O–Re=O backbone. The $[\{Re(O)Br(3,5\text{-}Me_2pzH)\}_2(\mu\text{-}O)(\mu\text{-}3,5\text{-}Me_2pz)_2]$ complex is only a minor product of the reaction of $[ReOBr_3(AsPh_3)(OAsPh_3)]$ with 3,5-$Me_2$pzH in acetone at room temperature [14]. The reactions of $[ReOX_3(PPh_3)_2]$ with bidentate and tetradentate ligands also result in the formation of dimers with a linear O=Re–O–Re=O unit (Section 2.3). The studies show dependence of these reactions on starting material, N-donor ligand, solvent and temperature, but water appears to be crucial also in the formation of dinuclear oxocompounds with a bent Re–O–Re core.

Fortin and Beauchamp found the relation between water percentage in acetone and the product of refluxing of $[ReOCl_3(biimMe_2)]$ in acetone. Refluxing of $[ReOCl_3(biimMe_2)]$ in acetone containing 5% water yields the $[\{ReOCl_2(biimH_2)\}_2(\mu\text{-}O)](PPh_4Cl)_2{\cdot}2H_2O$ with a linear O=Re–O–Re=O backbone, whereas the refluxing of $[ReOCl_3(biimMe_2)]$ in acetone containing less water (1%) leads to $[\{ReOCl_2\}_2(\mu\text{-}O)(\mu\text{-}biimMe_2)_2]$ [25].

The $[\{ReO[H(F)Bpz_2]\}_2(\mu\text{-}O)(\mu\text{-}pz)_2]$ complex was a product of refluxing of $[ReOI_2(Tp)]$ with an excess of NaF in acetonitrile in the air for 19 days. Reacting $[ReOI_2(Tp)]$ with NaF in the absence of air did not form $[\{ReO[H(F)Bpz_2]\}_2(\mu\text{-}O)(\mu\text{-}pz)_2]$, but produced two unidentified products [55].

The $[\{ReO[\eta^2\text{-}B(pz)_4]\}_2(\mu\text{-}O)(\mu\text{-}pz)_2]$ and $[\{ReO[\eta^2\text{-}B(pz)_4]\}_2(\mu\text{-}O)(\mu\text{-}3,5\text{-}Me_2pz)_2]$ complexes were obtained by two methods: (i) in the reaction of $[ReO(\mu\text{-}O)\{B(pz)_4\}]_2$ with pyrazole or 3,5-dimethylpyrazole, and (ii) during the slow recrystallization of $[\{ReO[\eta^2\text{-}B(pz)_4]\}_2(OMe)(pz)(pzH)]$ or $[\{ReO[\eta^2\text{-}B(pz)_4]\}_2(OMe)\text{-}(3,5\text{-}Me_2pz)(3,5\text{-}Me_2\text{-}pzH)]$, respectively. The formation of the above two complexes is difficult to explain, as all the species formed in the reactions were not identified [30].

The $[Re_2O_3(L^n)_2(PMe_2Ph)_2]$ complexes were isolated from the reactions of $[ReCl(N_2)(PMe_2Ph)_4]$ and $[ReCl(N_2)(PMePh_2)_4]$ with $HL^n$ ($n = 1, 2, 3$). Oxidation from Re(I) to Re(V) oxo-species by air was the more unexpected that oxo–Re(V) complexes with this class of ligands were never isolated when oxo- or dioxo-rhenium(V) precursors were used [56].

The interaction of $[ReOCl_4]$ with methanol and tertiary amine in diethyl ether leads to $[\{ReO(OMe)_2\}_2(\mu\text{-}O)(\mu\text{-}OMe)_2]$. The $[\{ReO(OMe)_2\}_2(\mu\text{-}O)(\mu\text{-}OMe)_2]$ complex can be also isolated by dissolution of rhenium in MeOH [57]. Addition of pyridine N-oxide to a toluene solution of $[\{ReO(Me)_2(PMe_3)_2\}(\mu\text{-}O)(\mu\text{-}CH_2)\{ReO(Me)_2\}]$ results in the isolation of $[\{ReO(Me)_2\}_2(\mu\text{-}O)(\mu\text{-}CH_2)]$ [58]. The rhenium peroxo $[\{ReO(H_2O)(O_2)_2\}_2(\mu\text{-}O)]$ seems to efficiently catalyze the oxidation of olefins, aromatics and certain organometallic compounds. It has been isolated from the system $Re_2O_7/H_2O_2$ in diethyl ether.

### 3.4. IR spectroscopy

The position of $\nu$(Re=O) and $\nu_{as}$(Re–O–Re) for the dinuclear complexes with a bent Re–O–Re unit are shown in Table 8.

The IR spectra of the dinuclear rhenium(V) complexes with a bent Re–O–Re core show one or two sharp bands in the range 894–968 $cm^{-1}$ assignable to the symmetric Re=O stretch and a strong $\nu_{as}$(Re–O–Re) band in the range 695–614 $cm^{-1}$. In comparison with the oxo rhenium complexes containing a linear O=Re–O–Re=O backbone, the $\nu$(Re=O) and $\nu_{as}$(Re–O–Re) bands are generally shifted towards the lower energy. The split of $\nu$(Re=O) band, observed for many complexes with a bent Re–O–Re system, is a consequence of the symmetry decrease.

The $\nu$(Re=O) bands of dirhenium(VI) complexes with a bent Re–O–Re core appear at much higher energy 970–1015 $cm^{-1}$. The position of $\nu_{as}$(Re–O–Re) band was given only for $[\{ReO(Me)_2\}_2(\mu\text{-}O)(\mu\text{-}CH_2)]$ (at 748 $cm^{-1}$).

### 3.5. UV–vis spectroscopy

Table 9 presents the positions and molar absorptivity of the electronic bands for the dinuclear rhenium(V) complexes with a bent O=Re–O–Re=O backbone.

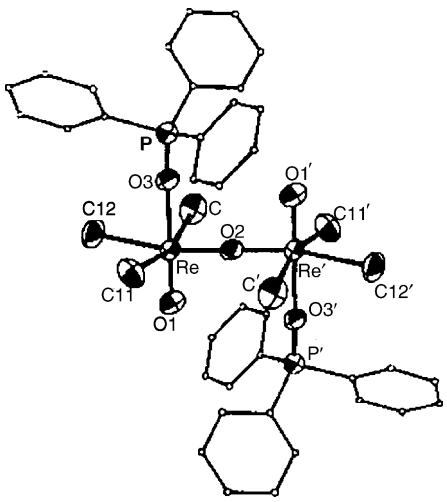


Fig. 21 Structure of. $[\{ReOCl_2(CH_3)(OPPh_3)\}_2(\mu\text{-}O)]$ [65].

Table 10
The selected bond lengths [Å] and angles [°] for the complexes with a linear Re—O—Re unit and *trans* arrangement of terminal oxo ligands

| Complex | Re—$O_t$ | Re—$O_b$ | $O_t$—Re—$O_b$ | Re—$O_b$—Re | Ref. |
|---|---|---|---|---|---|
| $[\{ReO(CH_3)_3\}_2(\mu\text{-}O)]$ | | | | | |
| Molecule I | 1.678(6) | 1.8514(9) | 115.6(3) | 180 | [63] |
| Molecule II | 1.674(6) | 1.850(6) | 113.9(3) | 178.8(4) | |
| | 1.672(6) | 1.851(6) | 114.8(3) | | |
| $[ReO\{(CH_3)_3SiCH_2\}_3](\mu\text{-}O)$ | 1.671(5) | 1.856(5) | 116.1(2) | 180 | [64] |
| $[\{ReOCl_2(CH_3)(OPPh_3)\}_2(\mu\text{-}O)]$ | 1.655(4) | 1.847(1) | | 180 | [65] |

The UV–vis spectrum of $[\{Re(O)Br(3,5\text{-}Me_2pzH)\}_2(\mu\text{-}O)(\mu\text{-}3,5\text{-}Me_2pz)_2]$ was discussed basing on the electronic transitions calculated using the time-dependent DFT method [45]. The following assignments of the experimental absorption bands of $[\{Re(O)Br(3,5\text{-}Me_2pzH)\}_2(\mu\text{-}O)(\mu\text{-}3,5\text{-}Me_2pz)_2]$ was made based on the results of the TDDFT calculations. The longest wave experimental band at 690.6 nm is of very low intensity and has d → d character. The absorption band at 300.0 nm corresponds to the transitions of π(Br) → d and π(pzH) → d character, and the band at 274.4 nm results from transitions of π(O)/σ(Br) → d and π(Br) → d and d → π*(pzH) origin. The experimental band 232.0 nm has MLCT character and corresponds to the transitions of d → π*(pz) character. In comparison with $[\{Re(O)Br_2(3,5\text{-}Me_2pzH)_2\}_2(\mu\text{-}O)]$, the experimental bands of $[\{Re(O)Br(3,5\text{-}Me_2pzH)\}_2(\mu\text{-}O)(\mu\text{-}3,5\text{-}Me_2pz)_2]$ corresponding to the electronic transitions of LMCT and MLCT character are shifted to higher energy. It results from higher energies of the unoccupied orbitals of $[\{Re(O)Br(3,5\text{-}Me_2pzH)\}_2(\mu\text{-}O)(\mu\text{-}3,5\text{-}Me_2pz)_2]$ in comparison with the corresponding MOs of $[\{Re(O)Br_2(3,5\text{-}Me_2pzH)_2\}_2(\mu\text{-}O)]$, whereas the energies of the corresponding occupied orbitals of these complexes are similar. The shortest wave experimental band of $[\{Re(O)Br(3,5\text{-}Me_2pzH)\}_2(\mu\text{-}O)(\mu\text{-}3,5\text{-}Me_2pz)_2]$ (at 222.2 nm) results from the transitions of LMCT ($n_N$ → d) character and LLCT (π(pz) → π*(pzH)) origin.

The UV–vis spectra of the complexes with a bent Re–O–Re core show low intensity bands in the range 700–580 nm and few much more intense absorption bands from 380 to 200 nm (Table 9). Basing on the results of TDDFT calculations for $[\{Re(O)Br(3,5\text{-}Me_2pzH)\}_2(\mu\text{-}O)(\mu\text{-}3,5\text{-}Me_2pz)_2]$, it can be assumed that the longest wavelength experimental bands of these complexes arise from the d→d transitions, the absorption bands at ∼220 nm are of LLCT (π → π*) origin, and the others have LMCT or MLCT character.

## 4. Complexes with a linear Re–O–Re unit and trans terminal oxo ligands geometry

Reports of the dinuclear rhenium complexes with a linear Re–O–Re unit and a *trans* arrangement of the terminal oxo ligands to each other are sparse, and the only structurally characterised complexes of this type appear to be $[ReO\{(CH_3)_3SiCH_2\}_3]_2(\mu\text{-}O)$ [64], $[\{ReOCl_2(CH_3)(OPPh_3)\}_2(\mu\text{-}O)]$ [65] and $[\{ReO(CH_3)_3\}_2(\mu\text{-}O)]$ [63]. The X-ray analysis of $[\{ReO(CH_3)_3\}_2(\mu\text{-}O)]$ revealed the presence of two crystallographically distinct molecules in the unit cell. The crystal structure of $[\{ReO(CH_3)_3\}_2(\mu\text{-}O)]$ is illustrated in Fig. 20.

Fig. 21 presents a perspective drawing of the $[\{ReOCl_2(CH_3)(OPPh_3)\}_2(\mu\text{-}O)]$ complex.

This geometry is typical of dinuclear rhenium(VI) complexes without any additional bridging ligands, except for an oxygen bridge. Table 10 presents the selected bond and angles for the dinuclear rhenium complexes with a linear Re–O–Re unit and *trans* arrangement of terminal oxo ligands. The two metal centers of $[\{ReO(CH_3)_3\}_2(\mu\text{-}O)]$ and $ReO\{(CH_3)_3SiCH_2\}_3](\mu\text{-}O)$ are pentacoordinated, and the coordination environment of the metal may be described in terms of either a distorted square pyramidal or a distorted trigonal bipyramidal geometry. In $[\{ReOCl_2(CH_3)(OPPh_3)\}_2(\mu\text{-}O)]$ two slightly distorted octahedra are joined linearly *via* an oxygen bridge. The Re–$O_b$ bond lengths of $[ReO\{(CH_3)_3SiCH_2\}_3](\mu\text{-}O)$, $[\{ReOCl_2(CH_3)(OPPh_3)\}_2(\mu\text{-}O)]$ and $[\{ReO(CH_3)_3\}_2(\mu\text{-}O)]$ are considerable shorter in comparison with the Re–$O_b$ distances found in the dinuclear complexes with a linear O=Re–O–Re=O backbone and a bent Re–O–Re core.

Electronic 'superexchange' in the structural Re–O–Re moiety with its shortened metal-oxygen bonds explains the diamagnetism of this $Re_2^{VI}$ compound.

$[\{ReO(CH_3)_3\}_2(\mu\text{-}O)]$ was prepared in high yield by the reaction of $(CH_3)_3SiOReO_3$ with trimethylaluminium in hexane solution [62]. In low yield it was isolated during the recrystallization of $(CH_3)_4ReO$ [61]. The formation of $[\{ReO(CH_3)_3\}_2(\mu\text{-}O)]$ from $[(CH_3)_4ReO]$ probably involves a slow reaction with aerial moisture proceeding through the formation of an initial complex with starting material, followed by the elimination of $CH_4$ to give $[(CH_3)_4ReO(OH)]$. Two molecules of hydroxo-complex condense together to afford $[\{ReO(CH_3)_3\}_2(\mu\text{-}O)]$.

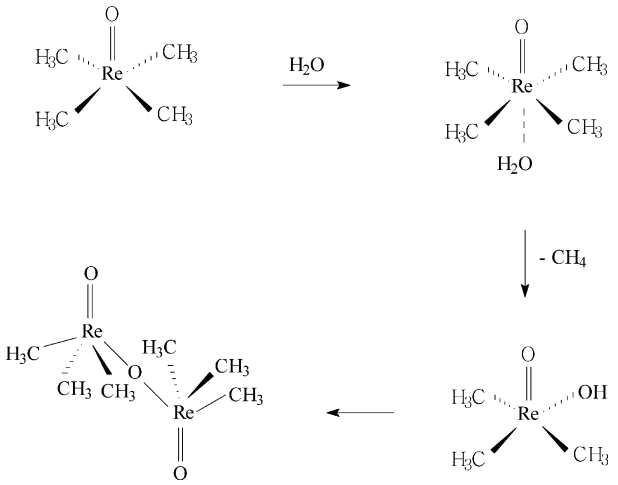


The [{$ReOCl_2(CH_3)(OPPh_3)$}$_2$($\mu$-O)] complex was obtained in the reaction of [$(CH_3)ReO_3$] with triphenylohosphane/trimethylchlorosilane.

## References


[1] J.R. Dilworth, S.J. Parrott, Chem. Soc. Rev. 27 (1998) 43.
[2] S.S. Jurisson, J.D. Lydon, Chem. Rev. 99 (1999) 2205.
[3] S. Liu, D.S. Edwards, Chem. Rev. 99 (1999) 2235.
[4] W.Y. Lin, C.P. Lin, S.J. Yeh, B.T. Hsieh, Z.T. Tsai, G. Tinbg, T.C. Yen, S.J. Wang, F.F. Knapp Jr., M.G. Stabin, J. Nucl. Med. 24 (1997) 590.
[5] J. Sattigeri, A.L. Rodriguez, J.A. Katzenellenbogen, Bioorg. Med. Chem. 10 (2002) 1381.
[6] E.S. Mull, V.H.R. Maxon, L.E. Schroder, L.C. Washburn, S.R. Thomas, R.C. Samaratunga, D. Biniakiewicz, J.S. Moulton, D.D. Cummings, G.J. Ehrhardt, V. Morris, J. Nucl. Med. 39 (1998) 659.
[7] A. Davison, A. Jones, Int. J. Appl. Radiat. Isot. 33 (1982) 875.
[8] P.J. Blower, J.R. Dilworth, J.P. Hutchison, T. Nicholson, J. Zubieta, J. Chem. Soc., Dalton Trans. (1986) 1339.
[9] (a) R.H. Holm, Chem. Rev. 87 (1987) 1401;
(b) C.C. Romão, F.E. Kühn, W.A. Hermann, Chem. Rev. 97 (1997) 3197.
[10] W.A. Hermann, F.E. Kühn, Acc. Chem. Res. 30 (1997) 169.
[11] (a) B. Jeżowska-Trzebiatowska, H. Kozłowski, L. Natkaniec, Bull. Acad. Polon. Sci., Sér. Sci. Chim. 13 (1965) 1;
(b) L. Szterenberg, L. Natkaniec, B. Jeżowska-Trzebiatowska, Bull. Acad. Polon. Sci., Sér. Sci. Chim. 10 (1976) 805;
(c) J.R. Campbell, R.J.H. Clark, J. C. S. Faraday II 76 (1980) 1103.
[12] C.J.L. Lock, G. Turner, Can. J. Chem. 56 (1978) 179.
[13] G. Backes-Dahmann, J. Enemark, Inorg. Chem. 26 (1987) 3960.
[14] B. Machura, J.O. Dzięgielewski, R. Kruszynski, T.J. Bartczak, J. Kusz, Inorg. Chim. Acta 357 (2004) 1011.
[15] E. Iengo, E. Zangrando, S. Mestroni, G. Fronzoni, M. Stener, E. Alessio, J. Chem. Soc., Dalton Trans. (2001) 1338.
[16] L.G. Marzilli, M. Iwamoto, E. Alessio, L. Hansen, M. Calligaris, J. Am. Chem. Soc. 116 (1994) 815.
[17] E. Alessio, E. Zangrando, E. Iengo, M. Macchi, P.A. Marzilli, L.G. Marzilli, Inorg. Chem. 39 (2000) 294.
[18] F.E. Hahn, L. Imhof, T. Lügger, Inorg. Chim. Acta 269 (1998) 347.
[19] C. Pearson, A.L. Beauchamp, Acta Crystallogr. C50 (1994) 42.
[20] S. Fortin, A.L. Beauchamp, Inorg. Chim. Acta 279 (1998) 159.
[21] T.I.A. Gerber, E. Hosten, Z.R. Tshentu, P. Mayer, E. Pérex-Carreño, S. Garcia-Granda, J.G.H. du Preez, J. Coord. Chem. 56 (2003) 1063.
[22] T. Głowiak, T. Lis, B. Jeżowska-Trzebiatowska, Bull. Acad. Pol. Sci., Ser. Sci. Chim. 20 (1972) 199.
[23] H.-J. Pietzsch, M. Reisgys, H. Spies, P. Leibnitz, B. Johannsen, Chem. Ber. 130 (1997) 357.
[24] H.-J. Pietzsch, H. Spies, P. Leibnitz, G. Reck, Polyhedron 14 (1995) 1849.
[25] S. Fortin, A.L. Beauchamp, Inorg. Chem. 39 (2000) 4886.
[26] Ch. Tessier, F.D. Rochon, A.L. Beauchamp, Inorg. Chem. 41 (2002) 6527.
[27] S.R. Fletcher, A.C. Skapski, J. Chem. Soc., Dalton (1972) 1073.
[28] G. Patsis, I. Pirmettis, Ch. Tsoukalas, M. Pelecanou, C.P. Raptopoulou, A. Terzis, M. Papadopoulos, E. Chiotellis, Inorg. Chim. Acta 342 (2003) 272.
[29] G. Battistuzzi, A.B. Corradi, D. Dallari, M. Saladini, R. Battistuzzi, Polyhedron 18 (1999) 57.
[30] A. Paulo, A. Domingos, I. Santos, Inorg. Chem. 35 (1996) 1798.
[31] K.J.C. van Bommel, W. Verboom, H. Kooijman, A.L. Spek, D.N. Reinhoudt, Inorg. Chem. 37 (1998) 4197.
[32] H. Kooijman, K.J.C. van Bommel, W. Verboom, D.N. Reinhoudt, J. Kroon, A.L. Spek, Acta Crystallogr. C56 (2000) 749.
[33] W.-T. Huang, J.-M. Lo, H.-H. Yao, F.-L. Liao, Acta Crystallogr. C56 (2000) 172.
[34] Cambridge Structural Database, Version 1.6 (2003).
[35] L. Hansen, Y.D. Lampeka, S.P. Gavrish, X. Xu, A.T. Taylor, L.G. Marzilli, Inorg. Chem. 39 (2000) 5859.
[36] K.J.C. van Bommel, W. Verboom, R. Hulst, H. Kooijman, A.L. Spek, D.N. Reinhoudt, Inorg. Chem. 39 (2000) 4099.
[37] M.R.A. Pillai, C.I. Barnes, E.O. Schlemper, Polyhedron 13 (1994) 701.
[38] P.O. Lumme, U. Turpeinen, Z. Stasicka, Acta Crystallogr. C47 (1991) 501.
[39] S. Bélanger, A.L. Beauchamp, Acta Crystallogr. C55 (1999) 517.
[40] H. Sugimoto, T. Takahira, T. Yoshimura, M. Shiro, M. Yamasaki, H. Miyake, K. Umakoshi, Y. Sasaki, Inorg. Chim. Acta 337 (2002) 203.
[41] S.I. Bartley, K.R. Dunbar, K.-Y. Shih, P.E. Fanwick, R.A. Walton, Inorg. Chem. 32 (1993) 1341.
[42] H.-F. Lang, P.E. Fanwick, R.A. Walton, Inorg. Chim. Acta 322 (2001) 17.
[43] J.M. Mayer, Inorg. Chem. 27 (1988) 3899.
[44] T. Takahira, K. Umakoshi, Y. Sasaki, Chem. Lett. (1994) 2315.
[45] B. Machura, M. Jaworska, in press.
[46] N.P. Johnson, F.I.M. Taha, G. Wilkinson, J. Chem. Soc. (1964) 2614.
[47] B. Machura, J.O. Dzięgielewski, R. Kruszynski, T.J. Bartczak, J. Kusz, Inorg. Chem. Commun. 6 (2003) 1436.
[48] L.A. Bottomley, P.E. Wojciechowski, G.N. Holder, Inorg. Chim. Acta 255 (1997) 149.
[49] F.A. Cotton, W.R. Robinson, R.A. Walton, Inorg. Chem. 6 (1967) 223.
[50] W.P. Griffith, T.D. Wickins, J. Chem. Soc. A (1967) 675.
[51] E. Alessio, L. Hansen, M. Iwamoto, L.G. Marzilli, J. Am. Chem. Soc. 118 (1996) 7593.
[52] B. Machura, J.O. Dzięgielewski, S. Michalik, R. Kruszynski, T.J. Bartczak, J. Kusz, Transit. Mater. Chem. 28 (2003) 939.
[53] K.P. Maresca, D.J. Rose, J. Zubieta, Inorg. Chim. Acta 260 (1997) 83.
[54] B. Machura, J.O. Dzięgielewski, R. Kruszynski, T.J. Bartczak, Polyhedron 22 (2003) 2869.
[55] D.D. DuMez, T.O. Northeutt, Y. Matano, J.M. Mayer, Inorg. Chem. 38 (1999) 3309.
[56] A. Lazzaro, G. Vertuani, P. Bergamini, N. Mantovani, A. Marchi, L. Marvelli, V. Roberto Rossi, V. Berolasi, Ferretti, J. Chem. Soc., Dalton Trans. (2002) 2843.
[57] W.A. Herrmann, J.K. Felixberger, J.G. Kuchler, E. Herdtweck, Z. Naturforsch, B. Chem. Sci. 45 (1990) 876.
[58] (a) P. Edwards, G. Wilkinson, K.M.A. Malik, M.B. Hurtshouse, J. Chem. Soc., Chem. Commun. (1979) 1159;
(b) P. Edwards, G. Wilkinson, M.B. Hurtshouse, K.M.A. Malik, J. Chem. Soc., Dalton (1980) 2467;

(c) G.A. Seisenbaeva, A.V. Shevelkov, J. Tegenfeldt, L. Kloo, D.V. Drobot, V.G. Kessler, J. Chem. Soc., Dalton Trans. (2001) 2762.
[59] D.M. Hoffman, D.A. Wierda, J. Am. Chem. Soc. 112 (1990) 7056.
[60] W.A. Herrman, J.D.G. Correia, F.E. Kühn, G.R.J. Artus, C.C. Romão, Chem. Eur. J. 2 (1996) 168.
[61] S. Trofimenko, Chem. Rev. 72 (1972) 497.
[62] S. Trofimenko, Inorg. Chem. 34 (1986) 115.
[63] L.J. Morris, A.J. Downs, J.C. Green, T.M. Greene, S.J. Teat, S. Parsons, J. Chem. Soc., Dalton Trans. (2002) 3142.
[64] P. Stavropoulos, P.G. Edwards, G. Wilkinson, M. Motevalli, K.M.A. Malik, M.B. Hursthouse, J. Chem. Soc., Dalton Trans. (1985) 2167.
[65] J.K. Felixberger, J.G. Kuchler, E. Herdtweck, R.A. Paciello, W.A. Hermann, Angew. Chem. Int. Ed. Engl. 27 (1988) 946.